# Chicken Feather Fibre Mat/PLA Composites for Thermal Insulation

**A thesis submitted in fulfilment**

**of the requirements for the degree**

**of**

**Master of Engineering**

**at**

**The University of Waikato**

**by**

**Xin Qin**


THE UNIVERSITY OF
WAIKATO
*Te Whare Wānanga o Waikato*

**February, 2015**

# Abstract

In order to add more economic value to chicken feather, a waste material of the poultry industry, it has been researched to incorporate chicken feather fibre (CFF) into resin to produce value-added composites. In the present research, chicken feather fibre was separated from the rachises and used to produce fibre mats. Then fibre mats were incorporated into polylactic acid (PLA) to make composites with low thermal conductivity. The procedure for making chicken feather fibre mat using an automatic dynamic sheet former was explored. Two different composite fabrication methods were investigated. One involved fabricate composite samples by hot pressing chicken feather fibre mats with PLA sheet. The other involved making composite specimens by hot pressing PLA powder and chicken feather fibre mats. A decrease in tensile strength compared to PLA had been expected before composite specimen fabricating according to previous research and so alkali treated fibre mats were used to improve tensile strength of composites.

It was concluded that chicken feather fibre mats with uniform quality could be made by controlling the jet-to-spin ratio and water wall thickness of the dynamic sheet former cylinder. Stable mat/PLA composites could be fabricated by hot pressing chicken feather fibre mats with PLA powder. Results from tensile testing indicated that alkali treatment could improve tensile strength to a small degree. SEM image analysis revealed that poor interfacial bonding between fibre barbs and PLA matrix had occurred. Thermal conductivity testing demonstrated improved thermal insulation with addition of CFF to PLA.

# Acknowledgements

I have many people to thank for the support I acquired throughout my Master's study.

First, I would like to thank my parents for their encouragement throughout my life. I would like give my deepest and honest thanks to my academic supervisor Professor Kim Pickering for giving me the greatest patience and most helpful academic support.

I would like to thank the large scale laboratory manager Chris Wang for training me and giving me a lot of instruction.

I would like to thank the MAPE technicians who provide the technical assistance for my research, especially Yuanji Zhang and Helen Turner.

I would like to thank Dr. Michael Duke, Dr. Alista Fow for helping me in my research.

I would like to thank the administrator Mary Dalbeth for her kindness and patience given to me.

I would like to thank the other composites group members namely Aruan and Tan for advice for my research.

# Table of Contents

# List of Figures

# List of Tables

# Chapter 1:

# Introduction

# Chapter 1:

# Introduction

Each year a large amount of chicken feathers, which are a waste material of the poultry industry, are produced overseas and within New Zealand. Poultry processers in the United States generally dispose of feather waste by burning or disposing at a landfill site. In New Zealand, chicken feathers are rendered to feather meal which sells for $569-622 per tonne. However, feather meal as a feed stock lacks methionine, histidine and lysine, which are essential nutrients for animals and as a fertiliser it contains excess nitrogen [13]. Incorporating this kind of low value agricultural waste product into polymers is an attractive solution to waste disposal which could create additional economic gains.

## 1.1 The Concept of Composites

The term composite，as defined in the Oxford English Dictionary, refers to something made up of several parts or elements. In the field of materials science, a composite or a composite material is a solid material composed of two or more separate components which contribute to its unique properties. Commonly, this consists of fibrous or particulate material contained within a phase referred to as the matrix. For example, a mud brick reinforced with straw is a type of composite material. The straw in the mud brick retains its original structure and acts as reinforcement to improve the strength of the mud brick. The mud matrix mainly binds the straw and provides a continuous material in three dimensions. The matrix phase of a composite may be metal, polymer or ceramic, however,

polymer-matrices composites are by far the most common due to their associated ease of manufacture, low cost and good performance and these are the focus of this thesis.

## 1.2 Development of Fibre-Reinforced Polymer Matrix Composites

### 1.2.1 General Composites

Following the advent of commercial glass fibre in 1930s, glass fibre reinforced resins came into the world. This new group of materials made by the engineers of Douglas Aircraft, an US based manufacturer, was intended to resolve a bottleneck in making of metal moulds for its sheet forming process [1]. Douglas engineers had been trying to employ cheap and easily fabricated plastic moulds to replace metal moulds that were expensive and had long lead times. Eventually, dies made of glass fibre reinforced phenol formaldehyde resin turned out to be successful due to the high strength of such composites contributed by glass fibres. Nowadays, researchers have improved mechanical strength of polymers to a higher level. LW H Leonard et al. have produced E-type glass fibre reinforced unsaturated thermosetting polyester (SYNOLAC 3317AW) with tensile strength more than six times the neat resin (Table 1.1).

**Table 1.1 Improvement in Mechanical Properties by Incorporating Glass Fibre into Polyester [2].**

| Properties | Materials | |
|---|---|---|
| | **Unsaturated thermosetting polyester (SYNOLAC 3317AW)** | **E-type glass fibre/ SYNOLAC 3317AW composite (60 wt% fibre content)** |
| Tensile strength (MPa) | 50 | 325 |
| Young's modulus (GPa) | 3.5 | 12.9 |
| Elongation at fracture (%) | 0.013 | 0.022 |

In addition to high strength, glass fibre reinforced resins have characteristics as follows: high corrosion resistance, radar transparent and electric insulation. As a consequence, glass fibre reinforced resins have been employed to fabricate pipes for delivering corrosive fluids and gases in the chemical and oil industry during the 1940s. Besides being applied in the public sector, glass fibre reinforced resins were used to make radomes (dome like hoods for protecting radar antennas) in the defence industry.

Invention of carbon fibre in 1961 was important for composites' development. Following that, resins reinforced by carbon fibres were used in the aerospace industry. The Beech Starship aircraft produced in the 1980s was the first civilian aircraft extensively using carbon fibre reinforced composites as its airframe materials. Nowadays, 50wt% of the Boeing 787 Dreamliner structure is made of composites where approximately 33 tons are carbon fibre reinforced composites [3], supporting carbon fibre reinforced composites to be strong and reliable. Carbon fibre reinforced composites also play an important role in improving fuel

efficiency because of mass reduction possible with their use, which is due to the high strength to weight ratio of carbon fibre composites [4].

### 1.2.2 Bio-composites

As the composite industry has continued to grow, an environmental problem associated with disposal of composite waste has come to public consideration. Due to their multiple phases and the difficulty of separation of these phases, recycling at the end of their usable lifetime is more challenging than treatment for pure plastics. As a result, end-of-life composite materials are generally landfilled or incinerated, but both landfill and incineration have negative influences on the environment.

A lot of effort has been made to explore substitutes for traditional inorganic filler reinforced composite materials in order to reduce environmental impact. One approach is to use bio-derived natural fibres with comparable specific strength to glass fibres as the reinforcement in composite materials. One advantage of using natural fibres is that the energy needed in their life cycle is considerably lower than that consumed during the life cycle of glass fibre as shown in Table 1.2 with hemp fibre as an example natural fibre.

**Table 1.2 Energy Schedule for Hemp Fibre and Glass Fibre Used in Composites [5].**

| Quantity (1 metric ton) | Hemp fibre | Glass fibre |
|---|---|---|
| Energy consumption in hemp fibre cultivation or glass fibre production (MJ) | 2060 | 48330 |
| Energy required for incineration (MJ) | 1700 | 1720 |
| Energy released during incineration (MJ) | 16390 | - |
| Energy balance (MJ) | 12630 produced | 50050 consumed |

Another benefit is that natural fibres are combustible, which makes their disposal at end-of-life easier and cheaper. On these grounds, natural fibre reinforced composites have been extensively studied and some prototypes as well as commercial products have been engineered especially in the automobile industry.


**Figure 1.1 Lotus Eco Elise with Hemp-fibre Reinforced Composite Panels [6].**

One application has been the engineering of Lotus Eco Elise (Figure 1.1), a prototype car with full scale use of hemp-fibre reinforced resins as its exterior panels. The high strength to weight ratio of hemp-fibre reinforced resins created a decrease in the entire mass of the car and improved both accelerating and braking performance, as well as fuel efficiency. Additionally, the high corrosive resistance enhanced the service performance of the car.

On a commercial scale, natural fibre reinforced resins have been used as internal components in vehicles. For example, FlexForm Techologies, a U.S. located company, has been supplying non-woven bast fibre-based composite mats to many vehicle manufacturers around the world. These mats are hybrid fabrics composed of bast fibres and thermoplastic fibre and can be subsequently moulded into semi-products (Figure 1.2). Their products have been utilized to produce a variety of components for vehicles including interior door panels, rear packaging trays, centre consoles and seat backs.

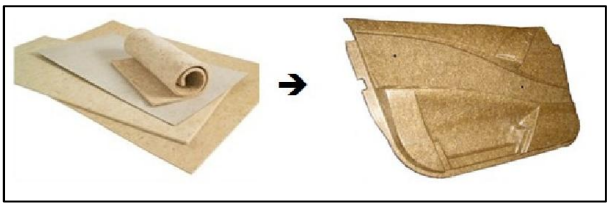

**Figure 1.2 Flexform Non-woven Mats and Compressed Hardboards (Left) and A Hot-pressed Interior Door Panel (Right) [7].**

Besides hemp fibres, other natural-organic fillers have also begun to find application as well. Among these, some examples are cotton, flax, sisal, kenaf, jute, starch [8]. Compared to plant fibre reinforced composites, research on composites filled with animal-based fibres, such as silk and wool, has been relatively less extensive. This is because most research has been conducted to improve material strength by incorporating natural fibres, while the animal-based fibres have relatively lower strength compared to plant fibres (Table 1.3).

**Table 1.3 Properties of Natural Fibres in Relation to Those of E-glass [9] [10] [11] [12].**

| | Density, g/cm$^3$ | Tensile strength, MPa | E-modulus, GPa | Elongation at break, % | Water absorption, % |
|---|---|---|---|---|---|
| E-glass | 2.55 | 2400 | 69 | 3 | - |
| Hemp | 1.48 | 550-900 | 50-70 | 1.6 | 8 |
| Jute | 1.46 | 600-1100 | 10-30 | 1.8 | 12 |
| Sisal | 1.33 | 600-700 | 38 | 2-3 | 11 |
| Flax | 1.4 | 800-1500 | 60-80 | 1.2-1.6 | 7 |
| Cotton | 1.51 | 400 | 12 | 3-10 | 8-25 |
| Kenaf | - | 930 | - | - | - |
| Silk | 1.3-1.4 | 200 | 0.5 | 15 | 8 |
| Wool | - | 120-170 | 2 | 25-35 | - |
| CFFs | 0.89 | 100-200 | 3-10 | - | - |

### 1.2.3 Chicken Feather Fibre (CFF) Reinforced Composites

Baron et al. conducted research on characterizing the mechanical properties of CFFs/polypropylene (PP) with different concentrations of coupling agent (MaPP-maleic anhydride grafted polypropylene) [14]. The tensile strength of PP was improved to 29 MPa from 25 MPa when reinforced with 20 wt% CFFs and 4% MaPP. Baron et al. have also published a report on the mechanical properties of CFF reinforced high-density polyethylene (HDPE) under different manufacturing conditions; it was found that the strength of composites was lower than neat PE [15].

With a rise in the price of the crude oil and the increasing demand for sustainable development as well as reducing the environmental impact of materials, fully bio-derived composites, or green composites have come into public consideration. Green composites are a type of bio-composite consisting of matrices and natural fibres both derived from biological resources [9]. PLA is the most studied and broadly commercialized bio-based polymer with worldwide PLA capacity estimated to rise from 401 million pounds a year in 2011 to 1.6 billion pounds in 2020 [16]. However, there are still some disadvantages including poor thermal resistance, inferior moisture resistance and brittleness which all hinder a widespread acceptance of this material in a variety of industries. One method to improve the performance of PLA is to incorporate fibres into it. CFF has been studied as reinforcement for PLA, but poor interfacial bonding has resulted in a decrease in strength with addition of CFF [17].

# 1.3 Innovative Applications for CFF

In New Zealand, chicken feathers have been processed to feather meal as a livestock feed, including as a substitute for fishmeal in aquaculture feed, or fertiliser by a rendering plant based in the Waikato region, but they still have the potential to be more valuable by being incorporated into polymers.

At the University of Waikato, researchers in the Polymers and Composites Research Group (PCRG) under Professor Kim Pickering have been exploring the use of a fibre sheet forming machine to make plant fibre mats with aligned fibres for enhancing the strength of polymers. Justification is provided by the expected degree of reinforcement shown for different orientations in Table 1.4, which is higher for orientated fibres. In fact, the PCRG has found that fibre mats made of hemp fibres or harakeke fibres are uniform and sufficiently stable for composite production. Hence, it was also attractive to explore what kind of product can be made with CFF using this machine.

**Table 1.4 Reinforcement Efficiency of Fibre-reinforced Composites for Several Fibre Orientations and at Various Directions of Stress Application [18].**

| Fibre orientation | Stress direction | Reinforcement efficiency |
|---|---|---|
| All fibre parallel | Parallel to fibres | 1 |
| | Perpendicular to fibres | 0 |
| Fibres randomly and uniformly distributed within a specific plane | Any direction in the plane of the fibres | 3/8 |
| Fibres randomly and uniformly distributed within three dimensions in space | Any direction | 1/5 |

Ye and Broughton have conducted research using chicken feather as a fibre source for nonwoven insulation [19]. They found that the feather fibre, in bonded batting form, appeared to be an effective insulating material. From this, it is assumed that if CFFs can be fabricated into mats by the sheet former, it could be possible to use them as composite fillers to reduce thermal conductivity of resins. The thermal conductivity of a material means the ability to conduct heat. Heat transfer occurs at a higher rate across materials of high thermal conductivity than across materials of low thermal conductivity. It can be seen in Table 1.5 that feathers have a lower value of thermal conductivity than some chemical insulation materials such as fibreglass and mineral wool insulation materials.

**Table 1.5 Thermal Conductivity of Selected Materials [20] [21].**

| **Materials** | **Thermal conductivity W/(m.K)** ***25*** **ºC** |
|---|---|
| Fibreglass | 0.040 |
| Mineral wool insulation materials | 0.040 |
| Polyurethane foam | 0.030 |
| Wool | 0.039 |
| Feathers | 0.034 |
| General insulation materials | 0.035-0.160 |
| PLA | 1.2-1.3 |

As a rapidly developed bioplastic, PLA was chosen as the matrix in the present research. PLA is currently used in packaging and food service ware, and is increasingly becoming the material of choice for more demanding applications in automotive, electronics and textiles [22]. Corbion, a corporation based in the Netherlands, have claimed they have produced high heat resistance PLA which can withstand temperatures of 100 - 140ºC which makes it ideal for hot beverage cups. It also allows manufacturers to replace oil-based plastics such as polystyrene

(PS) and polypropylene (PP) [23]. Based on these properties, CFF mats have the potential to improve the heat insulation of this kind of PLA to extend application to such as thermos flask, thermos lunch box, cooler box, etc.

However, as described above, incorporating CFFs into PLA could lead to a decrease in the tensile strength, which is undesirable. In order to assess how much CFFs would impair the mechanical strength of PLA and how much CFFs could improve insulation of PLA, research has to be done.

## 1.4 Research Objectives

This research aims to fabricate and characterize CFF mat/PLA composites to explore the feasibility of using this kind of composite for applications requiring thermal insulation. Based on this, the research is divided into the following objectives:

- Develop a procedure to make CFF mats
- Develop a fabrication method for CFF mat/PLA composites
- Characterize composite samples by thermal conductivity measurements, tensile testing and Scanning Electron Microscope (SEM) analysis.
- Analyse the results and identify which steps can be improved.

# Chapter 2:

# Literature Review

# Chapter 2:

# Literature review

## 2.1 Chicken Feather

Chicken feather is an abundant and cheap resource. Chickens are the most commonly raised domesticated birds worldwide and there is a large amount of chicken feather waste being produced every year. In 2010, for example, the US poultry industry produced about 22 million tonnes of broiler chickens with about 2 million tonnes of chicken feathers as waste product [24]. In New Zealand, about 180,000 tonnes of chicken meat was produced in 2013, according to the statistics from the poultry industry association NZ, which means about 20,000 tonnes of feather waste were made [25]. Annually, more than half of this is collected by a rendering plant owned by the Wallace Corporation, based in the Waikato region, New Zealand, where chicken feathers are processed into feather meal, which sells for about $0.50 per kilogram [26].

A review on the morphology, structure, constitution and properties of chicken feather used to assist the design and analysis of experiments in the present research follows.

### 2.1.1 Chicken Feather Morphology

Feathers make up about 8.5% of a chicken's mass and function as an epidermal covering for poultry, protecting it from damage, water and cold. Not all these

functions are performed by a single type of feather; there are in fact five kinds of feathers including contour, plumule, filoplume, chick down and bristle feather (Fig. 2.1).

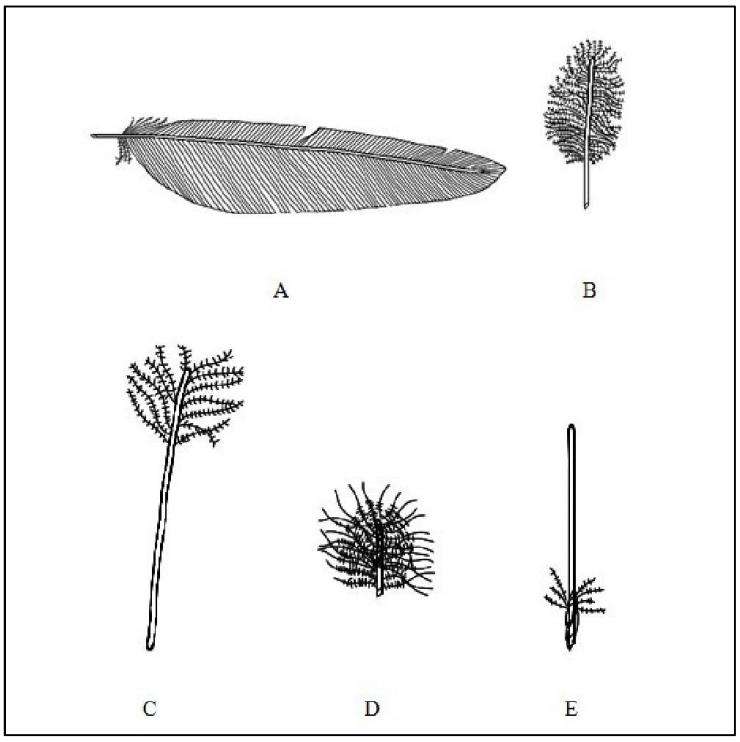


**Figure 2.1 Types of Chicken Feather: (A) Contour Feather, (B) Semiplume, (C) Filoplume, (D) Chick Down and (E) Bristle [27].**

## Contour Feathers

Contour feathers are the largest amongst these five kinds of feathers. Although as domestic fowl, chickens have adapted to living on the ground, they preserve the main features of contour feathers which is designed to assist flight. As shown in Figure 2.2, the contour feather consists of a central, stiff shaft with soft vanes on each side. The central shaft, on which the vanes are fixed, is called the rachis. The section of the rachis without vanes on it is sometimes referred to as the calamus (or quill). The vanes are made up of a lot of parallel barbs and much smaller

barbules and barbicels which interlock to form a stable configuration. It can help to understand the feather structure if the shaft is described as an analogy of trunk of a tree, while the barbs are the primary branches with secondary branches (barbules) on them, and the barbicels are tiny hook like twigs protruding from the barbules.

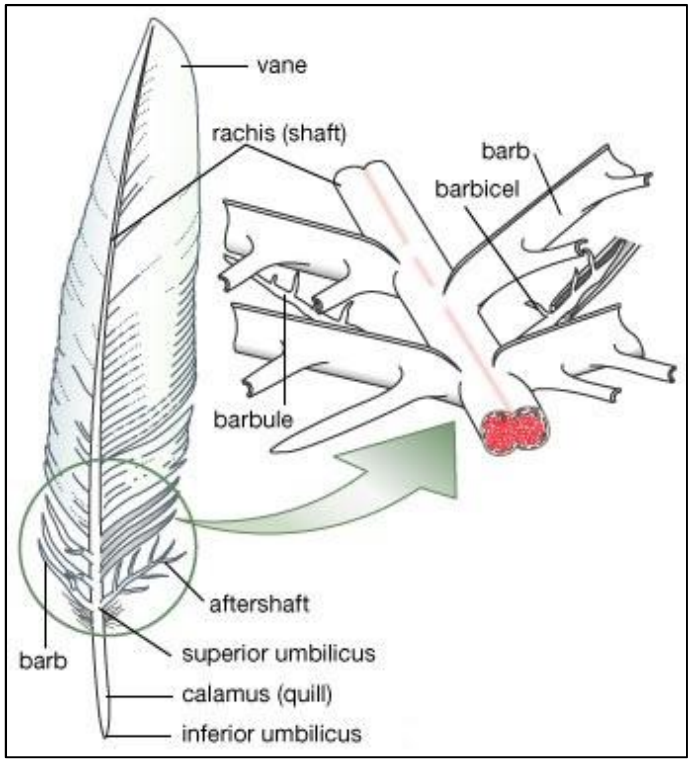


**Figure 2.2 Typical Contour Feather Structure [28].**

**Semiplume Feathers and Chick Down**

The semiplume and chick down feathers are found between contour feathers, providing insulation and streamlined shape for the birds. They do have barbules but lack barbicels to hold them together. Thus, the semiplume and down feathers look fluffy [27].

**Filoplume**

The structure of filoplume feathers are simpler compared to that of the previously described feathers. Filoplumes just have isolated barbs on the end of the rachis. However, there are plenty of nerve endings on filoplumes to sense and facilitate control the position of contour feathers [27].

**Bristle**

Bristle feathers found around a chicken's eyes and beak also provide tactile feedback, similar to whiskers on a dog or cat [29].

**Microstructure**

Much of the available information on feathers is focussed on contour feathers. For these feathers, the rachis has a diameter up to around 3mm at its widest part but it decreases away from the calamus. Barbs have a length of up to 35mm and a diameter of 40-400μm. The diameter of barbules ranges from 10μm to 30μm and they are less than 1mm long. Huda and Yang reported the fibre aspect ratio for barbs and barbules as 212 and 61 respectively [30]. Barbs and barbules are sold commercially as feather fibre used to reinforce polymers.

Chicken feather barbs have a honeycomb shaped hollow structure as can be seen in Fig. 2.3. Hence, CFF reinforced composites have the potential to be used in applications where materials which can absorb sound or retard heat transfer are desired [31]. Sound dampening of CFF composite has been researched by Huda et al. Chicken feather composites have been found to have more than twice the sound dampening properties of jute composites [30]. However, no research on insulation of CFF composite has been found in the literature. The honeycomb structure has been found to provide high resistance to compressibility [31].

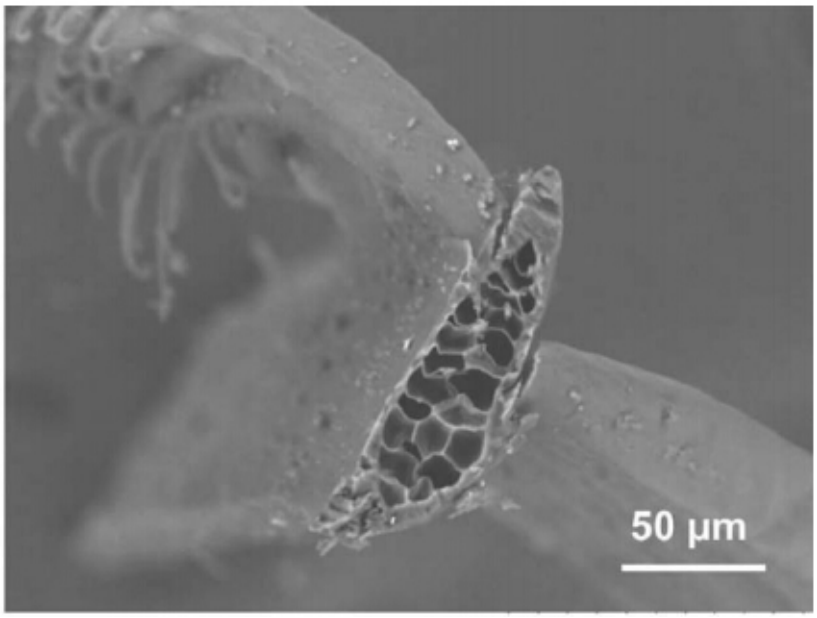


**Figure 2.3 SEM Image of the Cross-section of a Chicken Feather Barb [32].**

## 2.1.2 Feather Constituents

Chicken feathers are composed of more than 90wt% protein (keratin), approximately 1wt% lipids, and 8wt% water [13]. Keratin contains two kinds of conformations: α-helices and β-pleated sheets. The calamus has more β-pleated sheets than α-helices, whereas, the feather fibre derived from barbs and barbules has slightly more α-helices than β-pleated sheets. This leads to two different crystalline melting points of 240ºC and 230ºC for the barbs/barbules and calamus respectively [33].

Composition in terms of amino acid content is shown in Table 2.1. The content of cysteine, which is present in the largest quantity, is about 17.7wt%. Cysteine is the provider of thiol groups which can interact to form disulfide bonds contributing to the semi-crystalline structure of feather keratin [35]. It is also hydrophobic. The second largest quantity amino acid in chicken feather is serine

( 11.7wt% ) which contains the -OH group making it hydrophilic. Overall, the total content of hydrophobic amino acids in chicken feather is about 49.2wt%, while the fraction of hydrophilic amino acids is 50.8wt%. Hence, chicken feather fibre possesses hydrophobic and hydrophilic character in most equal amounts.

**Table 2.1 Amino Acid Content of Chicken Feather Fibre [34].**

| **Amino acid** | **Weight content (%)** | **Polarity** |
|---|---|---|
| Cysteine | 17.7 | Non-polar |
| Serine | 11.7 | Polar |
| Glutamic acid | 11.1 | Polar |
| Threonine | 6.9 | Polar |
| Glycine | 6.5 | Non-polar |
| Leucine | 6.1 | Non-polar |
| Valine | 5.9 | Non-polar |
| Arginine | 5.6 | Polar |
| Aspartic acid | 5.0 | Polar |
| Alanine | 4.8 | Non-polar |
| Proline | 3.6 | Non-polar |
| Isoleucine | 2.7 | Non-polar |
| Tyrosine | 1.9 | Polar |
| Phenylalanine | 1.4 | Non-polar |
| Histidine | 0.8 | Polar |
| Methionine | 0.5 | Non-polar |

Lipids (or preen oil) are another important component in feathers, which are fatty acids and secreted by preen glands to maintain the feather properties of waterproofing and colour. Lipids can hinder interaction with resin matrices resulting in bad interfacial adhesion.

## 2.1.3 Properties of Chicken Feather

**Mechanical Properties**

The mechanical performance of CFFs is primarily determined by their semi-crystalline structure. Zhan obtained mean values of the strain at break of 6.93%, tensile modulus of 3.59 GPa and tensile strength of 203±74 MPa for untreated barb fibre [32]. Reddy found that chicken feather fibres had strength of 1.4 grams per denier (180 MPa) and a tensile modulus of 36 grams per denier (4.7 GPa) for untreated intact barbs from contour feathers [31]. However, the tensile strength of CFFs reported by Ganesh ranged from 38 to 190 MPa [36]. One possible reason for the different results is that Ganesh's fibres were treated by hydrogen peroxide and sodium hypochlorite, which could have destroyed the fibre's structure. Another possible reason is that Ganesh used all kinds of fibres from different parts of chicken feathers.

**Thermal Stability**

Thermogravimetric analysis (TGA) of CFF has been carried out by Dullaart. This has shown a decrease of 5% in mass from about 25ºC to 55ºC due to the loss of free water and a second dramatic decline of weight at about 220ºC due to the decomposition of CFF [37]. These results suggest that the drying temperature for CFF should be above 55ºC, while the processing temperature for CFF reinforced composite should be controlled below 220ºC.

# 2.2 PLA

## 2.2.1 Lactic Acid-monomer

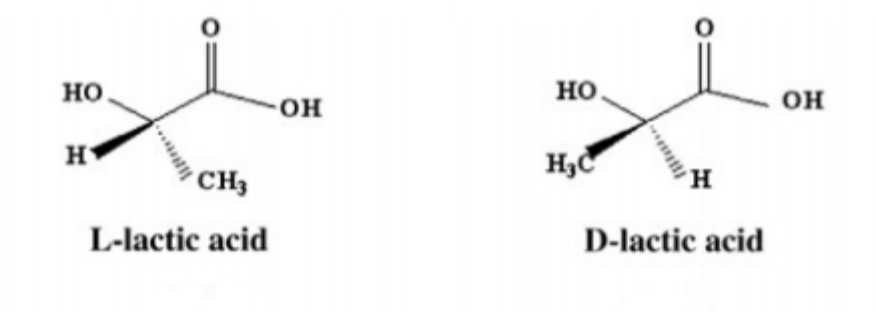


**Figure 2.4 Stereoforms of Lactic Acid [39].**

Lactic acid is the monomer from which PLA is produced. It has two stereo isomers, named L-lactic acid and D-lactic acid, as shown in Fig. 2.4. Either chemical synthesis or fermentation can be used to produce lactic acid. In chemical synthesis, a mixture containing both D- and L-lactic acid is produced by hydrolysing lactonitrile. In fermentation, either pure L- or pure D-lactic acid can be produced by using appropriate bacteria [39]. Besides the high product specificity, this bio-technique has some advantages including low cost, environmental friendliness, using renewable resources.

## 2.2.2 Ring-opening Polymerization

PLA is a type of polyester that can be produced through a polycondensation reaction between lactic acid monomers. Nevertheless, the molecular weights produced via the conventional polycondensation of lactic acid are not high enough and further polymerization is necessary to produce high molecular weight PLA.

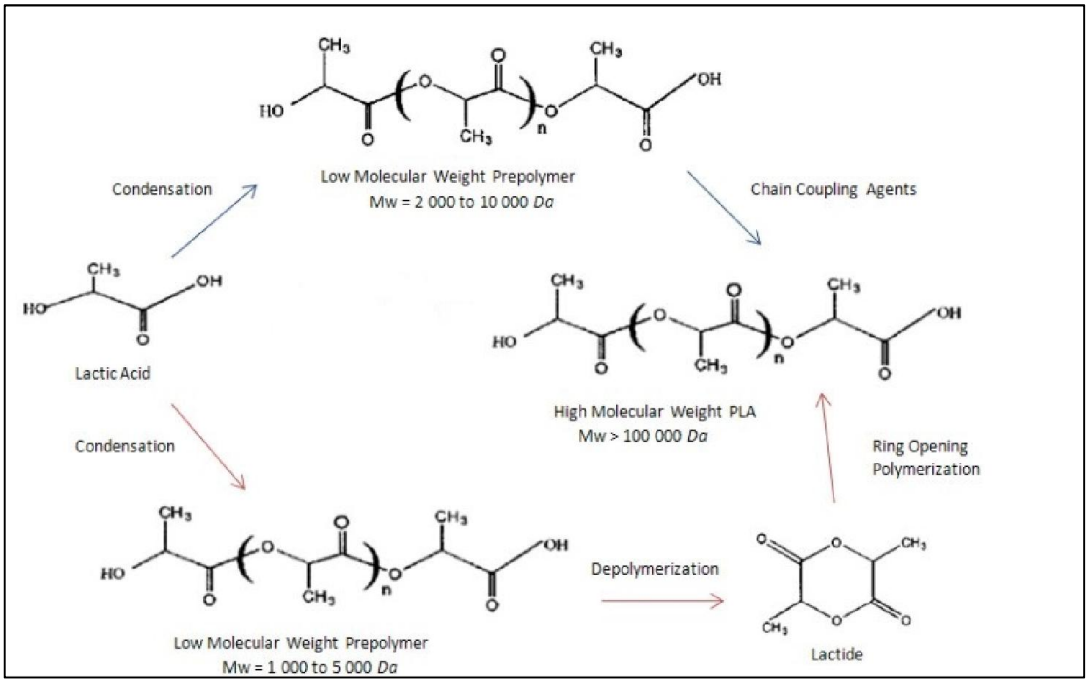


**a**

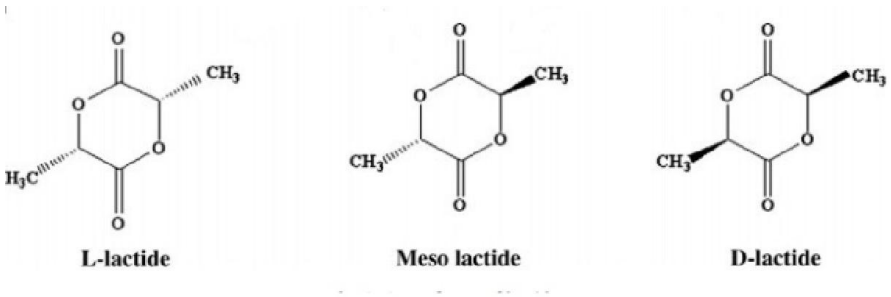


**b**

**Figure 2.5 a-Synthesis Methods for High Molecular Weight PLA, b-Stereoisomers of Lactide [38][39].**

Currently, the prevalent method to obtain PLA with satisfactory molecular weights is by ring-opening polymerization of lactide (Fig. 2.5a). In ring-opening polymerization, lactide, a cyclic lactic acid dimer, is an important intermediate, which is produced by catalytically depolymerizing the low molecular weight PLA [39]. Lactide has three kinds of stereoisomers including L-lactide, D-lactide and meso lactide as shown in Fig. 2.5b. Purified L-lactide, D-lactide, or meso-lactide dimer is catalytically polymerized to the corresponding high molecular weight

polyester [39]. The property of PLA made from different lactides varies considerably. Pure L-lactide or D-lactide can be converted into high crystalline PLA whereas meso lactide will produce an amorphous polymer [40]. The PLA glass transition temperature can vary from 50ºC to 80ºC and melt temperature can range from 130ºC to 180ºC with a variety of isomer composition [41].

## 2.3 Obtaining Fibre from Chicken Feathers

### 2.3.1 Decontamination and Cleaning of Chicken Feathers

For the present research, chicken feathers were obtained from a local rendering plant; these feathers required processing to remove microbes, blood and effluent in them for health and safety reasons as well as composite quality. Researchers at the University of Waikato have established a standard procedure to sterilize and clean raw chicken feathers [24]. In summary, the raw feathers collected from the Wallace Corporation were sterilized with NaOCl solution and $H_2O_2$ solution for further cleaning followed by testing for bacteria of concern for chicken feathers. Three potential pathogens on chicken feathers were recommended for monitoring, including Salmonellae, Campylobacter and Enterobacteriaceae [13]. It can be seen, from Table 2.2, that no Salmonellae were detected even in untreated feather and Campylobacter and Enterobacteriaceae were removed from the raw feathers. Furthermore, the fetid odour of raw feathers was eliminated.

**Table 2.2 Bacterial Test Results for Feather Treatment [13].**

| Sample ID | Untreated feather | Decontaminated feather | Cleaned feather |
|---|---|---|---|
| Salmonellae in 100 ml | Not detected | Not detected | Not detected |
| Campylobacter in 100 ml | C.jejuni detected | Not detected | Not detected |
| Enterobacteriaceae cfu per ml | 20,000 | 23 | <1 |

## 2.3.2 Comminution of Chicken Feathers

In general, comminution is a method used to reduce particle size, but in regard to processing chicken feathers comminution is conducted to separate barbs from the rachis of a feather. A standard process to comminute chicken feathers has been also created by researchers at the University of Waikato [24].


**Figure 2.6 Chicken Feather Comminution Apparatus.**

This has involved development of apparatus including delivery pipes, a pump, a feedstock tank, a pressure screen and a recovery filter (Fig. 2.6). The pump forces feather slurry to circulate within the system. A blade inside a 1-mm pressure screen is set at a certain torque to cut barbs from feathers. Barbs below a certain size are able to cross the screen to an accept stream whilst residues remain in a reject stream to return to the tank for further circulation. A triple-layered cheese cloth is used to filter CFFs from the accept stream. After running the system for 4 hours, the wet accepted fibres and wet rejected feathers were oven dried at 60ºC overnight. The dry accepted fibres and dry rejected feathers are shown in Fig. 2.7.

**Figure 2.7 Dry Accepted CFFs (left) and Dry Rejected CFs (right) [24].**

## 2.4 Issues Regarding Thermal Conductivity of Materials

Thermal conductivity (units W/(m·K)) is an important characteristic for thermal insulation materials, which quantifies their effectiveness in heat conduction. Thermal conductivity is a function of service temperature and moisture content of a material [65].

### 2.4.1 Insulation Materials

Thermal insulation materials are those that can retard the rate of heat flow across them. They are commonly applied as building materials to decrease the energy demands of heating and cooling systems as well as coatings for heated fluid pipes to minimize energy loss.

Heat transfer takes place through conduction, convection and radiation, hence, thermal insulation materials should be designed to prevent or retard these processes. The conventional method of improving insulation is to trap air in the materials to improve heat resistance, which occurs by reducing heat transfer by all mechanisms. The dead air-cells (closed air spaces) impede convective heat transfer by preventing air from moving. Creating small air-cells within thermal insulation materials across which the temperature difference is not large also reduces radiation [65]. Heat transfer by conduction is also slowed due to the very low thermal conductivity of still air

Common industrial insulation materials, including fibreglass, mineral wool and polyurethane insulation, are all non-biodegradable and unsustainable. However renewable and environmentally friendly natural fibre insulation materials have been developed to meet demands in some developed countries such as UK, France and Germany [66]. These include sheep wool insulation battings, flax insulation mats and hemp insulation mats. Though CFF has also been researched with regard to its insulation properties, a proven commercially viable process for producing CFF has not been available [19]. This has limited the development of CFFs as insulation materials.

### 2.4.2 Natural Fibre Filled Insulation Composites

Liu et al. explored the use of forestry and agricultural residues (pine and rice straw) for manufacturing thermal insulation products. Polyurethane was sprayed onto pine wood fibres and rice straw to form prepregs. The prepregs were then injection moulded into products. The new bio-based materials developed in this work had good thermal insulating properties with potential for application in buildings as insulating materials [67].

Takagi et al. have researched PLA-bamboo fibre composites. Bamboo fibres were mixed with PLA resin to form preforms and composites were produced by hot pressing. The thermal conductivity of this composite was approximately equal to that of wood of the same density [68].

### 2.4.3 Factors Affecting Composites Thermal Conductivity

The thermal conductivity of a fibre reinforced composite is determined mainly by the thermal conductivity of both the matrix and the fibre reinforcement themselves, the volume fraction of each orientation of the fibre reinforcement and the interfacial adhesion between the fibre and the matrix [42]. The matrix and reinforcing fibre themselves determine the maximum possible thermal conductivity of composites [71]. The influences of other factors have been theoretically estimated through a computer model established by Marcos-Gómez et al. [42].

## Interfacial Adhesion and Reinforcement Volume Fraction

The interface effect has been considered by Marcos-Gómez through replacing the reinforcements and the non-ideal interface around them with an 'effective' reinforcement with the thermal conductivity, $K_r^{eff}$, given by [42]

$$K_r^{eff} = K_r/(1 + K_r/ha) \quad 2\text{-}1$$

where $K_r$ is the reinforcement thermal conductivity, *a* is the reinforcement radius and *h* the interfacial thermal conductance. When the interfacial adhesion is poor, the interfacial thermal conductance *h* will be low and result in a low $K_r^{eff}$. This relationship has been incorporated into a model established by Hasselman and Johnson to describe overall composite thermal conductivity [42]. Fibre orientation for this model was neglected and the composite thermal conductivity, $K_c$ was proposal to be obtainable by:

$$\frac{K_c}{K_m} = \frac{\varphi^{eff}(1+2V_f)+(2-2V_f)}{\varphi^{eff}(1-V_f)+(2+V_f)} \quad 2\text{-}2$$

where $K_m$ is the matrix thermal conductivity, $V_f$ is the reinforcement volume fraction and $\varphi^{eff}$ is the ratio of the effective reinforcement thermal conductivity and the matrix thermal conductivity $\frac{K_r^{eff}}{K_m}$.

Equation (2-2) can be transformed to

$$\frac{K_c}{K_m} = \frac{3\varphi^{eff}+6}{(1-\varphi^{eff})V_f+\varphi^{eff}+2} - 2 \quad 2\text{-}3$$

Assuming the composite has a perfect interface, then $K_r^{eff}$ equals the reinforcement thermal conductivity $K_r$.

So

$$\varphi^{eff} = \frac{K_r^{eff}}{K_m} = \frac{K_r}{K_m} \qquad 2\text{-}4$$

Thus $K_r < K_m$ means $\varphi^{eff} < 1$ and in equation (2-3) $K_c$ decreases with an increase in the value of $V_f$.

## Orientation of Reinforcement

Generally, fibres with hollow structure have different thermal conductivity in the longitudinal and transverse directions such as carbon nanotubes and hemp fibres. For carbon nanotubes, a longitudinal thermal conductivity of 3000 W/mK and a transversal thermal conductivity of 6 W/mK are typical values [42]. For hemp fibres, Behzad found that the longitudinal and transversal thermal conductivity of hemp fibres were 1.45 W/mK and 0.16W/mK respectively [72]. The thermal conductivity of composites reinforced by hemp fibres has been shown to depend on the orientation of hemp fibres. Behzad reported that thermal conductivity of composites decreased with increase in fibre volume fraction when the reinforcing fibres were parallel to the heat flow direction, but when the reinforcing fibres were perpendicular to the heat flow direction, the thermal conductivity of composites increased with increase in fibre volume fraction. This was because the thermal conductivity of matrix used in Behzad's research was intermediate to the longitudinal and transversal thermal conductivity of hemp fibres.

Chicken feather fibres are also anisotropic with hollow features extending longitudinally along the feather axis (Fig. 2.3). It is supposed that there is a difference between its longitudinal and transversal thermal conductivity. However,

no related research has been carried out to provide actual values of the different thermal conductivity.

## 2.5 Factors influencing Composite Mechanical Strength

The reinforcing fibres in polymer matrix composites can be either continuous or short. Common continuous fibres include glass, carbon and aramid fibres. The tensile strength of continuous-fibre reinforced composites has a theoretical maximum value given by $V_m\sigma_m + V_f\sigma_f$ according to the Rule of Mixtures and a minimum value $(\frac{V_m}{\sigma_m} + \frac{V_f}{\sigma_f})^{-1}$, where $\sigma_m$ is the tensile strength of the matrix, $\sigma_f$ is the tensile strength of the fibres, $V_m$ is the matrix volume fraction, $V_f$ is the fibre volume fraction. When all continuous fibres are unidirectional, the tensile strength of composites reaches a maximum value in the fibre axial direction and reaches the minimum value in the transverse fibres direction. When continuous fibres randomly align, the tensile strength of composites is expected to lie between these maximum and minimum values.

For short fibres such as chopped glass fibre, graphite, cellulose-based fibre and chicken feather fibre, the Modified Rule of Mixtures can be used to predict the tensile strength of short fibre reinforced composites, which is given as follows [44]:

$$\sigma_c = V_m\sigma_m^* + V_f\sigma_f K_1 K_2 \qquad 2\text{-}5$$

where

$\sigma_c$= the tensile strength of the composite

$\sigma_f$= the tensile strength of the fibres

$V_m$= the matrix volume fraction

$V_f$= the fibre volume fraction

$K_1$= orientation factor

$K_2$= a factor dependant on the stress transfer between the matrix and the fibres

$\sigma_m^*$= the tensile contribution of the polymer matrix at the failure strain of the composite.

## 2.5.1 Effect of Fibre Orientation

Fibre orientation is a factor that influences the tensile strength of fibre reinforced composites represented by $K_1$ in Equation 2-5. The composite strength reaches a maximum value when the reinforcing fibres are aligned parallel to the direction of applied load, which can be seen in Table 1.4. The orientation of short fibres in composites during processing is commonly determined by the size of fibres, the viscoelastic properties of the melted polymer matrix, the mould dimensions and processing conditions [10]. Therefore, an appropriate grade of matrix, a suitable mould and optimised processing conditions should be considered to make fibres aligned parallel to the direction of applied load during processing.

## 2.5.2 Effect of Fibre Length

$K_2$ in Equation 2-5 depends on fibre length and interfacial strength. Length is a factor as short fibres are not uniformly loaded along their entire length. This is because load within a short fibre within a composite is built up by shear stress acting at the interface, such that the tensile load at its ends will be zero and

increase along the fibre length. Indeed, fibre of length below that termed the critical length, will not fracture when the composite is loaded, as a critical length is required to allow the load to build-up to give the failure stress (tensile strength) of the fibre. However, the critical length depends on both the inherent properties of fibre and the interfacial adhesion between fibres and matrices, which is given by [18]：

$$L_c = \sigma_f^* d/2\tau_c$$

where $\sigma_f^*$ is fibre tensile strength, $d$ is the fibre diameter, $\tau_c$ is the fibre-matrix bond strength (or the shear yield strength of the matrix, whichever is smaller).

## 2.5.3 Effect of Interfacial Bonding

As mentioned previously, the strength of the fibre-matrix interface is part of what is represented by $K_2$ in the Modified Rule of Mixtures is significant for the physical and mechanical properties of composite materials. A strong interface assures effective stress transfer between fibres and the matrix leading to good reinforcement. There are three types of interfacial bonding mechanisms which can work alone or collaborate to influence the interfacial strength of the type of composites of interest here [10]:

- Mechanical interlocking
- Interdiffusion bonding
- Chemical bonding

Among them, mechanical interlocking, chemical bonding and interdiffusion bonding are possible at the interface of polymer matrix composites.

## Mechanical Interlocking

Mechanical interlocking at the fibre/matrix interface occurs more readily when the fibre surface is rough and jagged. This type of bonding mainly leads to an increase in the interfacial shear strength and make slip between fibres and matrix less likely. For plant fibres, it is common to use alkali to pretreat the fibres in order to achieve a cleaner and rougher fibre surface [45]. Gassan et al. reported that alkali treatment of the jute fibre could lead to an increase in tensile strength and Young's modulus of the composite material, although this could also occur due to exposing more chemical groups or structure to allow chemical bonding or interdiffusion bonding [46].

For CFF composites, Supri Abdul Ghani et al. have also used alkali to treat CFFs and obtained alkali treated CFF reinforced composites with higher strength values than their untreated fibre counterparts [47]. Compared to untreated CFF, a rougher surface of treated CFF is observed in the research, which was believed to have contributed to enhanced interfacial adhesion between the fibres and the matrix.

## Interdiffusion Bonding

For interfaces involving polymers, interdiffusion bonding occurs when polymer chains from each component entangle and intertwine together [10]. This phenomenon may be considerable when the reinforcing fibre is compatible with the matrix. The strength of this bonding is related to the length of intertwined chains, the degree of entanglement and the number of chains per unit of area [10].

## Chemical Bonding

Chemical bonding occurs when functional groups on the fibre surface reacts with reactive chemical groups within the matrix. The effect of this type of bonding depends on the strength of per chemical bond and their numbers per unit area. There are two kinds of common chemical bonds, including covalent bonding, hydrogen bonding, and their strength are 200-800 kJ/mol, 10-40 kJ/mol respectively.

The most common method to create chemical bonding between fibres and matrices is to utilize coupling agents. Maleic anhydride polypropylene (MaPP) is a common coupling agent for fibre reinforced polymers to improve its mechanical performance. MaPP can react at one end with the hydroxyl groups on the surface of fibres to form strong covalent bonds. The other end of MaPP is a polypropylene chain which can entangle with the matrix during mixing. Pickering and Ji used MaPP A-C 950P to couple radiata pine fibre and polypropylene and obtained 177% and 123% improvement in Young's modulus and tensile strength respectively at 50% fibre with 3wt% MaPP [51]. Koppel used MaPP to enhance the tensile strength of CFF reinforced PP (50wt% fibre content) to more than 185% of that (50wt% fibre content) without MaPP [53]. Li reported an improvement from 12.4MPa to 24.4MPa and 3.23GPa to 4.35GPa in tensile strength and Young's modulus respectively at 70wt% wood fibre/polyethylene composites (fibres were obtained from a saw mill) with 3wt% MaPE [52].

Besides using coupling agents, polymers that are compatible with the matrix can be grafted onto some active sites of the fibre surface, such as, the thiol groups on cysteine amino acid and hydroxyl sections [48]. Martínez-Hernández et al. have obtained PMMA- grafted keratin fibres using a redox initiation system consisting of potassium permanganate, sulfuric acid and maleic acid [49]. Mu and Liu also

achieved PS-grafted horse hair via surface-initiated atom transfer radical polymerization [50]. These grafted groups can interdiffuse with the polymer matrix to enhance the strength of the composite materials.

### 2.5.4 Effect of Fibre Content

Changes in composite tensile strength with variation in fibre content can be generally predicted by Equation 2-5. However, at very low fibre fractions, tensile strength of composites commonly declines temporarily with increased fibre content due to bonds between the fibre and matrix breaking caused by high deformation [10]. At higher fibre fractions, the matrix is sufficiently restrained and the deformation of bonds reduces. When deformation reduces to a value that could be endured by the strength of bond between the fibre and matrix, the fibre content of this situation is known as the critical fibre fraction. At fibre content higher than the critical fibre fraction, the tensile strength of composites rises with an increase in fibre content. However, it is seen that when very high values (>60/70 wt%) of fibre content are used, composite strength decreases relative to that achieved at an optimum fibre content due to insufficient wetting of the matrix material, as seen by Nishino [54].

## 2.6 Fabrication of Short Fibre Reinforced Composites

The most widely used techniques for processing short fibres with thermoplastic polymers are injection moulding and compression moulding. Extrusion can also be used to produce short fibre reinforced composites, but it is most commonly

used to compound fibres and thermoplastic polymers for subsequent moulding process.

### 2.6.1 Extrusion

A twin-screw extruder is widely used to carry out extrusion as this gives high shear stress enabling thorough mixing. The feed stock can be melted, mixed and compressed in the extruder barrel, then shaped extrudate such as, threads, sheets and rods can be produced through a die connected with the extruder barrel. Afterward, the extrudate can then be chopped to granules and then moulded by an injection moulding machine.

### 2.6.2 Injection Moulding

Injection moulding is efficient in the production of consistent products but there still are disadvantages. One is that the fibre length will considerably reduce due to the high shear stress between fibres and viscous matrices during injection moulding (as also occurs in extrusion) [55]. Another is that it is hard to disperse fibres evenly in composites when the fibre content is relatively high. Both of these disadvantages will lead to a reduction in mechanical strength. The shear stress will also destroy internal fibre structure for fibres such as CFFs for which structure is important to its thermal insulation.

## 2.6.3 Compression Moulding

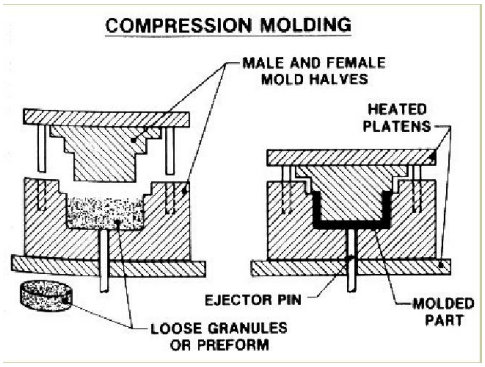


**Figure 2.8 Configuration of Compression Moulding [58].**

Compression moulding is another common method to fabricate short fibre reinforced polymers. During this process, a mixture of resins and fibres are placed into the cavity of a preheated mould [56]. The mould is then closed by bringing the male and female halves together, and desired pressure is applied on the mould to compress materials inside to fill the cavity of the mould (Fig. 2.8). The advantage is that composites with thermosetting resin matrix can be produced using this method.

The main disadvantage for compression moulding is that it takes considerable time to heat up and cool down the mould and hence makes the process more time-consuming. Steel moulds can be replaced with aluminium moulds to reduce the process period. A more efficient aluminium frame mould is used in Ben's research, which is illustrated in Fig. 2.9 [57]. Two Teflon sheets are laid between moulding material and the hot plates to prevent adhesion while the frame mould is used to control the sample dimension. This mould could considerably reduce the production cycle. However, pressure transferred to the moulding material would be limited.

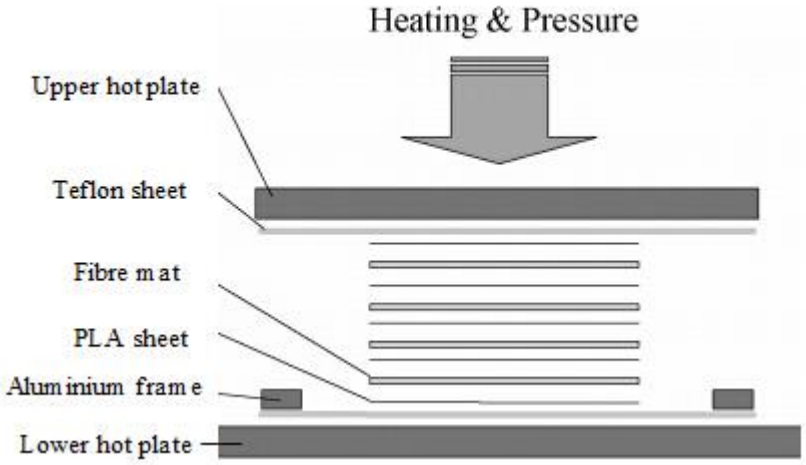


**Figure 2.9 Hot Press Moulding of Fibre Mat Composite [57].**

The duration of the mould bearing an applied pressure has a significant effect on composite properties. A short compression period can result in an insufficient impregnation, leading to poor interfacial bonding. Reversely, an excessively long compression period will do harm to the fibre structure, impairing the desired performance of the composites [57]. For CFF composites, not only the duration but also the value of the pressure can influence the composite properties. If a high pressure is applied on the mould, the hollow structure of CFFs will be destroyed, resulting in a significant reduction in the thermal insulation performance of the products. On the other hand, extremely low pressure may not be able to compress the matrix to wet fibre mats thoroughly, which results in a poor mechanical performance for the samples.

## 2.7 Production of Fibre Mats

As short fibre, CFF can be fabricated into mats by non-woven methods. It is hard to form a mat with CFF by common methods such as carding and needle punching.

However, it is possible to make mats using an automatic sheet former. A rapid Kothen sheet former has been used to fabricate hybrid CFF/cotton linter sheets [59]. This machine sucks fibre pulp through a disc-like sieve to form a randomly oriented fibre sheet on the surface of the sieve. The fibre orientation is in all direction in the sheet plane.

The other type of automatic sheet former is the Canpa automatic dynamic sheet former (ADSF) which can be used to fabricate either homogeneous or hybrid sheets. A hybrid sheet made by the Canpa automatic dynamic sheet former refers to a multiple-layer sheet. Each layer in a hybrid sheet is composed of one type of homogeneous fibres. When producing hybrid sheets, the size of the particles within feedstock pulp should be small enough to avoid blocking, because this was designed to use fine pulp as feedstock. The delivering tubes for the homogeneous sheet fabrication system are larger than those of hybrid sheet fabrication system, which permits feedstock pulp including larger particle such as CFFs to flow through. Hence, CFF mats are preferred to be fabricated in the homogeneous sheet fabrication system. Although this machine has not been mentioned in any research to be used for CFF mat producing, it has the potential to make CFF mats.

### 2.7.1 Canpa ADSF Configuration

A Canpa automatic dynamic sheet former can produce sheets by spraying the fibre pulp onto the porous inner layer cylinder surface (Fig. 2.10). The reciprocal movement of the nozzle and the spinning of the cylinder occur simultaneously to evenly distribute fibres. The inner layer is designed to support fibres and form wet sheets on its surface. A water wall is formed on the surface of the solid outer cylinder layer and at the same time covers the inner layer (Fig. 2.10). The function of the water wall is to provide enough water to disperse fibres thoroughly. Once wet sheets are formed, dewatering occurs through continued spinning of the

cylinder to make relatively dry and stable fibre mats. One of features of DSF is that it can fabricate sheets with fibres mostly aligned parallel to cylinder spinning direction by controlling the jet-to-spin ratio [60]. It is assumed that alignment will considerably improve the strength of composites in the fibre alignment direction.

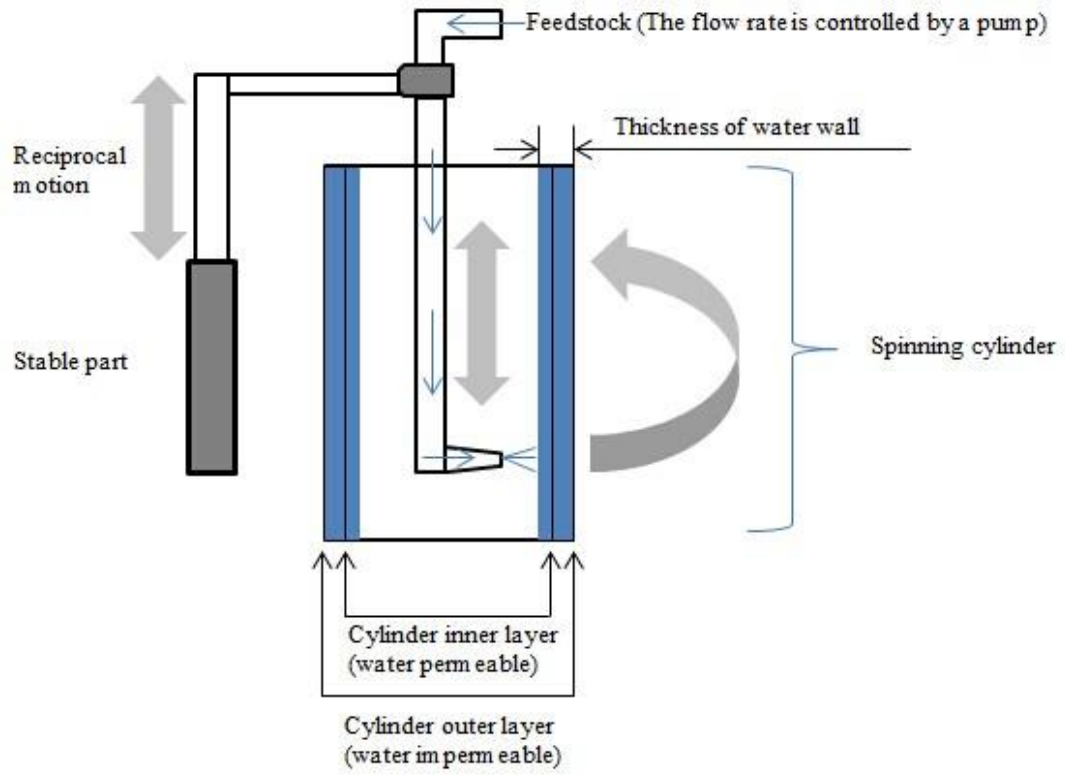


**Figure 2.10 Schematic of the DFS**

## 2.7.2 Key Parameters for the Canpa ADSF

There are eight controllable operating parameters in the Canpa automatic dynamic sheet former main menu, including layer, tank, stock, pump, wire, dwt, pwwl and swwl numbers as explained below:

- layer number is used to set the number of layers to be made.
- tank number is used to specify the source tank of stock for making a particular layer.
- stock number is used to control the total feed volume for making a particular layer.
- pump number sets the speed of the pump which decides the flow rate through the nozzle.
- wire number sets the spinning speed of the cylinder.
- dwt number controls the dewatering speed.
- Pwwl (primary water wall level) number which controls the amount of liquid that is introduced in the spinning centrifuge to build the initial water wall.
- swwl (secondary water wall level) number sets the limit of water wall thickness during the entire sheet making process and this function is performed by positioning the scoop during the spin of the centrifuge.

All of these are required for hybrid sheet fabrication, while the first three are not required for homogeneous sheet fabrication.

## 2.7.3 Jet-to-Spin Speed Ratio

Here the term jet refers to the fast pulp stream through the nozzle and spin refers to the spinning speed of the cylinder. The ratio of jet-to-spin speed determines the orientation of fibres in mats as explained below.

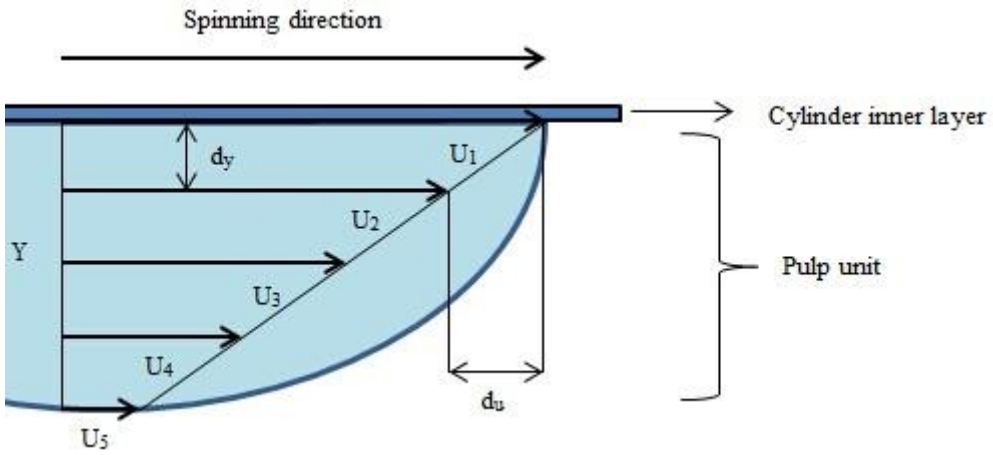


**Figure 2.11 Initial Velocity Gradient in Pulp on the Cylinder Inner Surface.**

Fig. 2.11 illustrates the initial velocity gradient state of pulp when it is jetted onto the inner surface of the spinning cylinder. This pulp can be regarded as Newtonian fluid and a velocity gradient occurs when it touches the spinning cylinder inner surface. There are shear forces (τ) existing between layers of fluid with different velocities, which is given by the Newtonian fluid equation as:

$$\tau = \mu \frac{d_u}{d_y} \qquad 2\text{-}6$$

where μ is the viscosity of the fluid.

In the pulp, the velocity gradient is:

$$\frac{d_u}{d_y} = \frac{U_5 - U_1}{Y} \qquad 2\text{-}7$$

where $U_5$ is the initial velocity of the pulp unit, which is determined by the jet force, $U_1$ is the spinning speed of the cylinder and $Y$ is the thickness of this pulp.

According to Equation 2-6 and 2-7, the shear force in pulp is equal to $\mu \frac{U_5 - U_1}{Y}$. Hence, when the difference between the jet pulp initiative velocity and the

cylinder spinning speed is bigger, the shear force in the jet pulp is larger and the fibres within it are more likely to align.

### 2.7.4 Thickness of Water Wall

There are a lot of tiny holes in the inner layer of the cylinder which permit water to go through and keep fibres on the inner side. It is necessary to build a water wall on the inner layer surface to provide a surrounding fluid to prevent the jetted pulp from drying on that surface during sheet making. An important parameter for that water wall is the thickness. If the wall is very thin, it is detrimental for fibres to disperse evenly in that water wall. On the other hand, the fibres tend to move to the bottom of the water wall if the thickness is large. This happens because the bottom thickness of the water wall is larger than that of the top due to the effect of gravity. If the water wall contains a large amount of water, then the difference in the thickness between bottom and top part is detrimental for making a uniform sheet. For CFF pulp, there is no relevant data for sheet making. Therefore, the proper thickness of water wall has to be investigated in experiments.

## 2.8 Thermal Conductivity Measurement

There are several standard methods for thermal conductivity measurement; among these the most common methods are:

- the guarded hot plate method
- the thin heater method
- the heat flow metre method.

All these methods need be conducted in a stead state condition, which means the temperature and heat flow readings are stable instead of changing with time or

fluctuating significantly.

## 2.8.1 Guarded Hot Plate Method

**Apparatus**

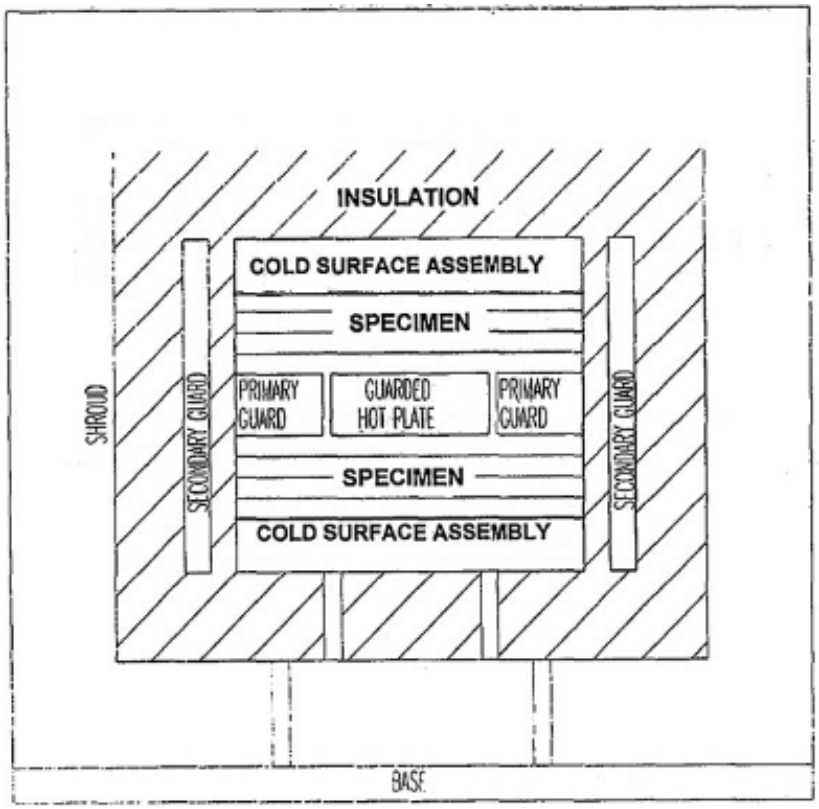


**Figure 2.12 General Arrangement of the Mechanical Components of the Guarded Hot Plate Apparatus [61].**

The ideal configuration for guarded hot plate measurement includes two isothermal cold surface assemblies and a guarded hot plate. The guarded hot plate is surrounded by two primary guard heaters with a defined distance to the central hot place in the horizontal direction. The test specimen is sandwiched between these units and all these elements are surrounded by insulation material as shown in Fig. 2.12.

**Principle**

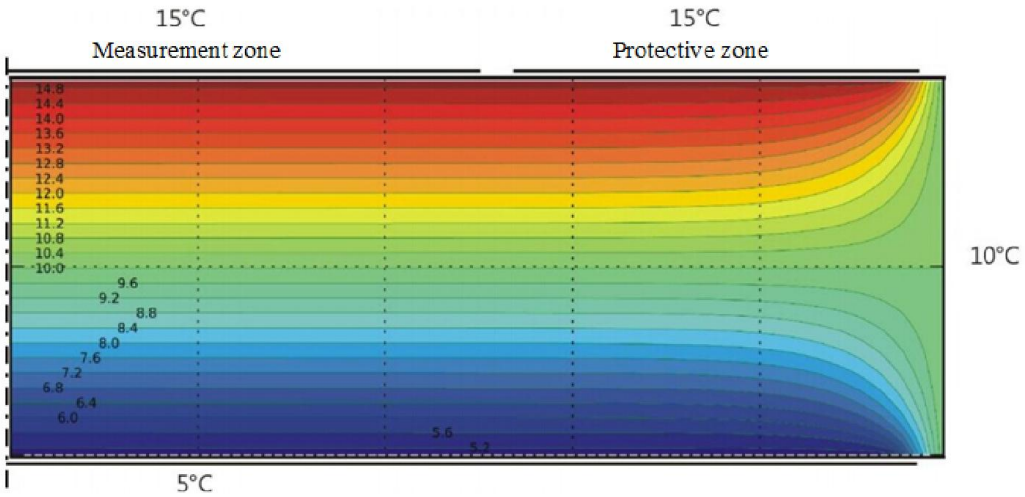


**Figure 2.13 Temperature Field within a Specimen in a Typical Guarded Hot Plate Apparatus [62].**

The measurement zone of the specimen in Fig. 2.13 is heated by the guarded hot plate in Fig. 2.12. The primary guards heat the protective zone to eliminate the temperature difference between the measured zone and the rest of the specimen in the horizontal direction. Hence, no horizontal heat flow happens during the measurement and the total consumed power of the guarded hot plate transfers across the measurement volume from the hot side to the cold side. By knowing the defined area of the guarded hot plate, the thickness of the sample and the precisely controlled and measured temperatures of the upper and lower surfaces of the specimen, the thermal conductivity can be calculated directly by the Fourier Law.

## 2.8.2 Thin Heater Method

**Apparatus**

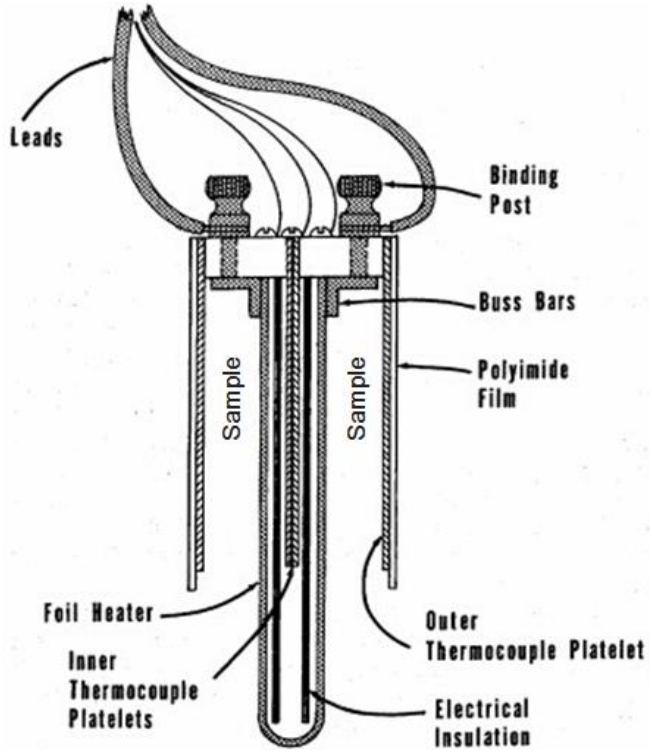


**Figure 2.14 Schematic of One Thin-Foil Heater Apparatus [63].**

The apparatus is mainly composed of a thin foil heater and inner and outer thermocouples. The thin foil heater (shown in Fig. 2.14) is a 0.03mm thick stainless steel foil and is uniform to within $\pm$0.2 % to ensure an even heat flow through samples [63]. The electrical insulation is made of 0.25mm thick silicon glass laminate to protect the inner thermocouple platelets in order to obtain an accurate inner temperature reading [63].

**Principle**

The foil heater is made sufficiently thin so that heat loss from its front and back edges is insignificant, and so that there is no need for isolation and separate

temperature control of a guard region [63]. The key uncertainty is that the power produced by the foil may lose to the air through samples' front and back surface, which will considerably influence the accuracy of eventual results. Hence, the dimension of specimens for this method should be exactly controlled to a limited thickness in order to reduce lateral heat loss of the samples.

## 2.8.3 Heat Flow Metre Method

**Apparatus**

There are three available configurations for the heat flow metre apparatus, as shown in Fig 2.15.

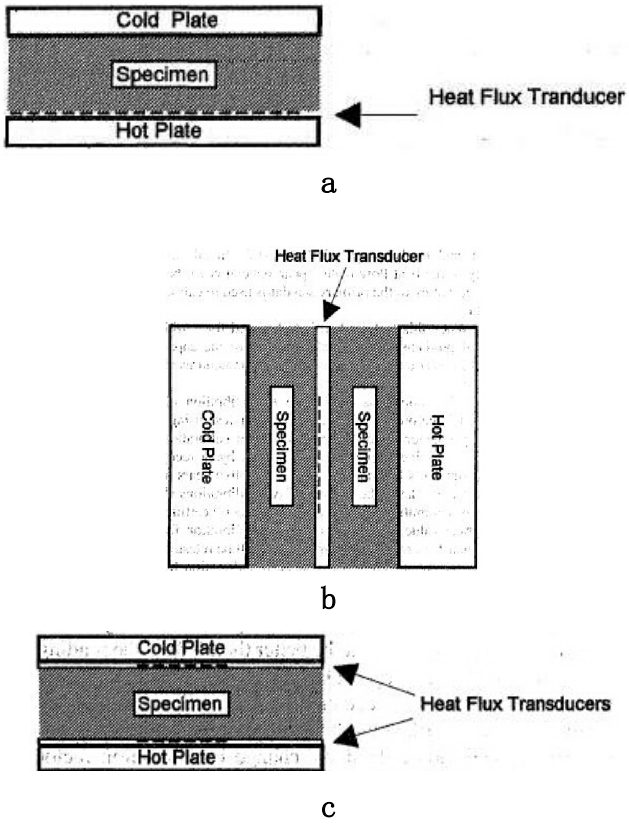


**Figure 2.15 Apparatus with a-One Heat Flux Transducer and One Specimen, b-One Heat Flux Transducer and Two Specimen, c-Two Heat Flux Transducer and One Specimen [64].**

All these configurations consist of two isothermal plate auxiliaries but different amounts of heat flux transducers and specimens. Theoretically, each configuration will yield the same result if measurement is conducted in a steady state conditions and the apparatus has been calibrated with a standard sample properly.

A transducer with a high thermal resistance is generally used when the transducer is attached to one or both of the isothermal plates [64]. The low-thermal resistance heat flux transducer is better suited to the configuration where the transducer is attached between two samples [64]. While considering the edge heat loss, the configuration with heat flux transducers mounted on isothermal plates is preferred due to the least sensitivity to edge heat loss in such case. If the thickness of the specimen is sufficiently small, configuration of Fig. 2.15-a is competent to provide an acceptable result.

**Principle**

Unlike the two previous methods, the heat flow is measured directly in this technique through a heat flux transducer. At the same time, the boundary temperature of both upper and lower sides of the sample should be measured with thermocouples. All the data obtained is valid only in the condition of a steady state. By measuring the thickness of the sample precisely, all variables which are needed to calculate the thermal conductivity of the sample through Fourier's Law are available [64].

# Chapter 3:

# Materials and Methods

# Chapter 3:

# Materials and Methods

## 3.1 Overview

The purpose of this research was to fabricate and characterize CFF mat/PLA composites to explore the feasibility to use CFFs to improve thermal insulation of PLA and as well research the effects of CFF mat content on both mechanical properties and the thermal conductivity of PLA. In order to achieve this objective, the following steps were covered in this research.

- Feather fibre acquirement
- CFF mat processing
- PLA sheet production
- Composite fabrication
- Thermal conductivity measuring
- Tensile testing
- SEM

Raw chicken feathers were obtained mixed with decaying skin and foul-smelling water, which contained a lot of pathogenic bacteria. They had to be sterilised and deodorized before any further processing. Once feathers were cleaned, CFFs could be separated from feather rachises through a pressure screen. Then CFF/water pulp with an appropriate concentration could be processed to produce wet sheets using a sheet former. These sheets were then oven dried resulting in loose mats. Composites were produced by compounding the fibre mats and PLA

in a mould by hot pressing. Composites were then cut into strips for tensile tests as well as thermal conductivity tests.

# 3.2 Chicken Feather Treatment

## 3.2.1 Materials Used

Raw chicken feathers were kindly provided by the Wallace Corporation, Waikato, New Zealand. Sodium Hydroxide (NaOH), sodium hypochlorite (NaOCl) and hydrogen peroxide were procured from Ajax Finechem Pty Ltd

## 3.2.2 Decontamination and Cleaning

Decontamination was carried out to kill pathogenic bacteria such as E. coli, salmonella and Campylobacter known to be present on raw poultry feathers. Initially 2.5kg of raw unprocessed feathers and 25L of water were added into a 30L Lamort pulp mixer with a flat disc agitator. A 1 molar solution of sodium hydroxide (NaOH) was then added to adjust the pH to 10 which was tested with pH 10-12 litmus paper. Finally, 250ml of sodium hypochlorite (NaOCl) 30% was added to the slurry; this was then mixed at 12Hz for 30 minutes. After mixing, the liquid was drained and feathers were rinsed with 25L of water. The decontamination process was repeated for a second time before the feathers were stored in a fridge at -4ºC awaiting hydrogen peroxide treatment.

Cleaning was carried out to eliminate any residual bacteria and remove odour and excess lipids. This step was also conducted in the 30L Lamort pulp mixer.

Disinfected feathers were added to the pulp mixer in batches of 2.5kg with 25L of water and 125ml of 15wt% hydrogen peroxide ($H_2O_2$) solution, which was mixed for 30 minutes at 12Hz. This process was repeated three times. Between each stage, liquid was drained and feathers were rinsed with 25L of water to ensure all contaminants were washed away. Once the cleaning process was completed the feathers were stored in a fridge at -4ºC awaiting comminution treatment.

## 3.3 Comminution of Chicken Feather

The apparatus shown in Fig. 2.6 was used to produce CFFs by separating barbs and barbules from feather rachises [24]. Initially, 300L water was added into the 600L tank, then the pressure screen was turned on with a torque of 80% and the main pump was set at 25Hz. The “accept” and “reject” valve values were set to 35% and 100% respectively. When the system was running steadily, 1.3kg wet feathers were slowly added over a ten minute period to the tank in order to reduce clumping on the water’s surface. A sieve was fixed under the output opening of the accept stream for fibre recovery. The fibres were collected from the sieve by hand through out the process to keep the sieve mesh clear enough for accept stream flowing through. Each comminution process was run continuously for 3 hours. Fibres recovered were oven dried at 60ºC overnight.

# 3.4 Production of Fibre Mats

CFF mats were made by using a Canpa automatic dynamic sheet former. As no other researcher has made CFF mats with ADSF before, different parameters and feeding amount were trialled to make appropriate CFF mats.

The important parameters for the ADSF to make CFF mats include the speed of the pump, spinning speed of the cylinder and thickness of water wall. Parameters were set as shown in Table 3.1.

**Table 3.1 Experiment Number and Parameters.**

| No. | PUMP value | WIRE value | SWWL value | Feeding Amount |
|---|---|---|---|---|
| 1 | 65 | 80 | 0 | 30g CFFs |
| 2 | 65 | 80 | 2 | 30g CFFs |
| 3 | 65 | 80 | 4 | 30g CFFs |
| 4 | 65 | 80 | 5 | 30g CFFs |
| 5 | 65 | 80 | 6 | 30g CFFs |
| 6 | 65 | 80 | 8 | 30g CFFs |
| 7 | 45 | 80 | 5 | 30g CFFs |
| 8 | 65 | 80 | 5 | 20gCFFs |
| 9 | 65 | 80 | 5 | 10gCFFs |

According to Section 2.7.3, the value of wire number should be as high as possible to provide the largest shear force in the pulp to align fibres. The highest value of wire number is 100, but in order to protect the machine the value was set to 80. The influence of swwl value was hard to predict and therefore experiments 1-6 were carried out to investigate the influence of swwl value on mat quality. Experiment 7 was designed based on the best swwl value from previous experiments (1-6) to trial the effect of pump value on mat quality. Experiments 8 and 9 were used to research the effect of feeding amount on mat quality.

It was hard to maintain CFF pulp on the surface of inner layer of the sheet former cylinder due to the large size of the holes in the cylinder inner layer. Hence, a Kevlar holding sheet was used to assist holding the CFF pulp. The weight ratio of CFF to water used in this section was 1:500.

## 3.5 Chicken Feather Fibre Treatment

Alkali treated CFF reinforced composites have been found to have higher tensile strength than untreated CFF composites according to Supri Abdul Ghani's research [69]. In the present research, CFFs were soaked in a 2 wt% solution of NaOH at room temperature for 2 hours. The fibre to solution ratio by weight was 1:100. In order to treat 30g CFFs, 60g analytical grade of NaOH was dissolved in 3L water. Then fibres were added into the NaOH solution and stirred for 2 hours. The fibres was then filtered and rinsed in warm flowing water for 2 minutes. Fibres were oven dried at 60ºC overnight.

# 3.6 Production of PLA Sheet

PLA polymer 3052D, from NatureWorks LLC, USA, via Convex Plastics was used as the matrix material. The PLA was provided in pellet form which is not directly suitable for fabrication of composites in the present research. PLA sheet production was carried out using a ThermoPrism TSE-16-TC twin-screw extruder at a screw speed of 120 rpm with the temperatures as shown in Fig. 3.1 and the sheet die shown in Fig. 3.2.


**Figure 3.1 Extruder Screw Temperature Set.**

**Figure 3.2 Sheet Die.**

The sheet die includes two heating elements and both were set to 170ºC. PLA sheet was cut to 15cm length then heated in an oven at 60ºC to flatten.

## 3.7 Fabrication of Composites with PLA Sheet and CFF Mats

PLA sheet/CFF mat composites were made using a KOTAKI hydraulic hot press. The mould was preheated in the hot press at 160ºC for 40 minutes. Both CFF mats and PLA sheet were cut to size (22×15cm) and oven dried overnight before fabrication. When producing composites, PLA sheets and CFF mats were stacked in the preheated mould as shown in Fig 3.3. The mould was returned to the hot press at 160ºC. After 8 minutes, the mould was pressed at 5 tons for 2 minutes. It was then removed from the press and allowed to cool under a load of 20kg before removing the composite.

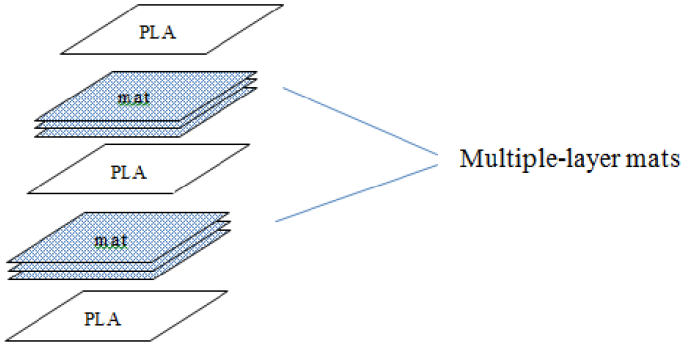


**Figure 3.3 Illustration of Stacking Structure.**

Two composites with different mat content were fabricated for tests, shown in Table 3.2 and Fig. 3.4. They both consisted of three PLA sheets separated by two multiple-layer mats. One comprised one PLA sheet + four layers of mat + one PLA sheet + four layers of mat + one PLA sheet. The other was one PLA sheet + eight layers of mat + one PLA sheet + eight layers of mat + one PLA sheet. They were named C4×2 and C8×2 according to respective mat content. Then they were cut to 15×1.5cm specimens waiting for tensile test.

**Table 3.2 Fibre Content of PLA Sheet/ CFF Mat Composites.**

| Composites | Amount of PLA sheets | Number of CFF mats | Fibre content wt% |
|---|---|---|---|
| C4×2 | 3 layers (123g) | 8 layers (16g) | 12% |
| C8×2 | 3 layers (125g) | 16 layers (36g) | 22% |

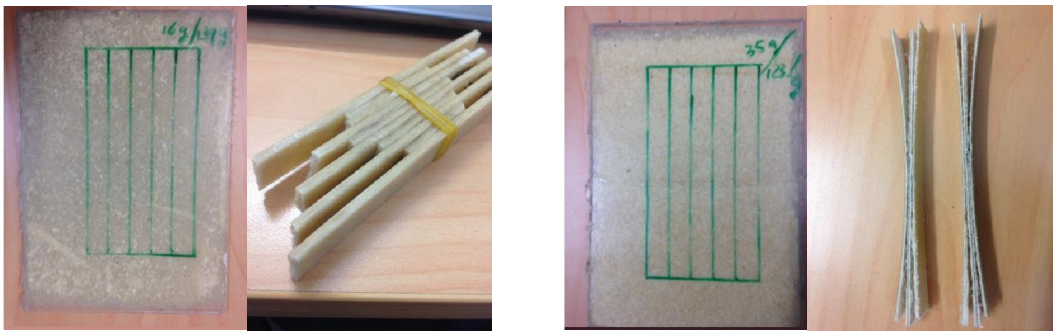

**Figure 3.4 Composite C4×2 (left) C8×2 (right)**

Samples with 12wt% fibre were stable enough to carry out tensile testing. However, the specimens with 22wt% fibre split along mats and therefore were not suitable for tensile testing.

# 3.8 Fabrication of Composites with PLA Powder and CFF Mats

In order to produce PLA/CFF mat composites with higher stability, PLA powder 3052D, from NatureWorks LLC, USA, via Convex Plastics was used to fabricate composites. PLA powder/CFF mat composites were made using KOTAKI hydraulic hot press machine. Three composites with different mat content were made. Each composite consisted of 100g PLA powder and different amount of CFF mats. They were configured as shown in Fig. 3.5 and named as PCA, PCB and PCC respectively.

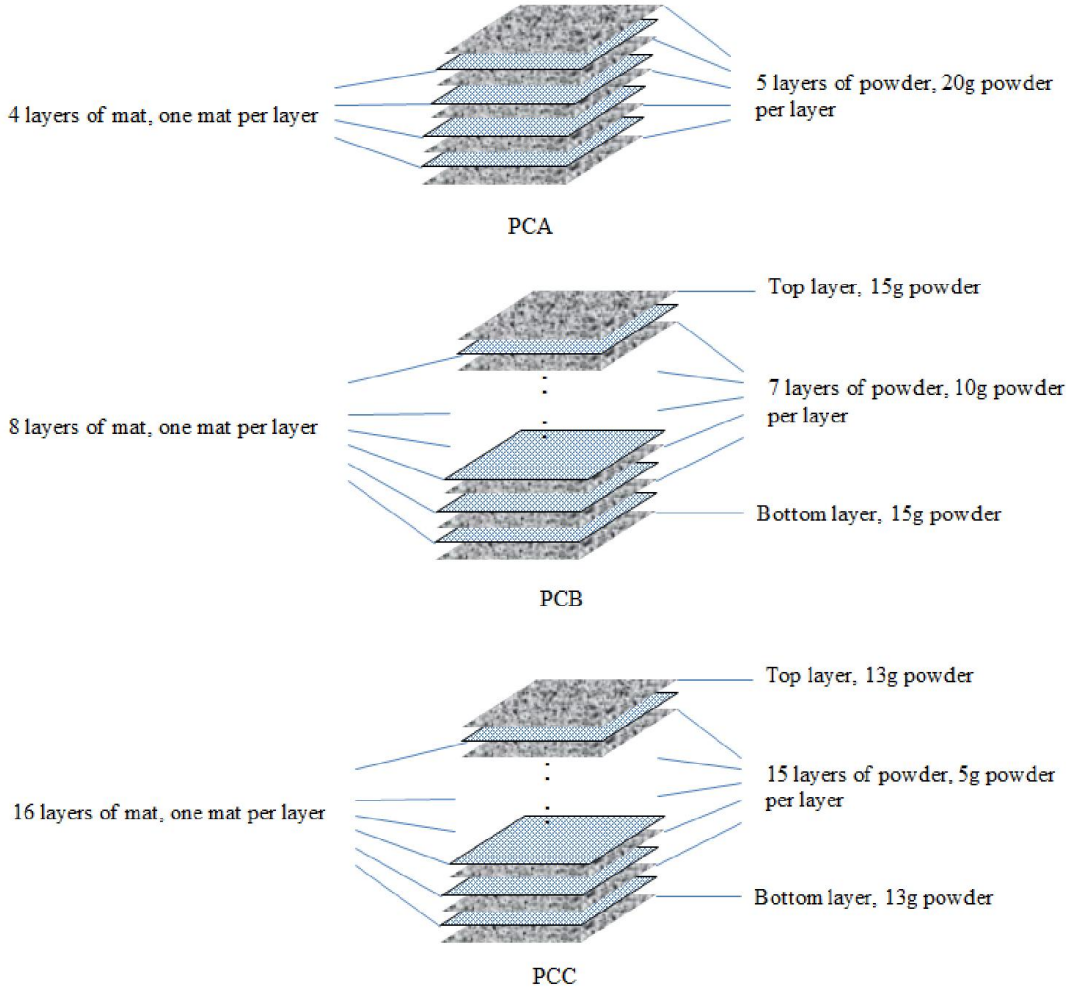


**Figure 3.5 PLA Powder/ CFF Mat Composite Profile.**

PLA powder and CFF mats were manually added into a cold mould (22×15cm) according to the profile in Fig. 3.5 and then were heated in the hot press at 160ºC for 40 minutes. Afterwards, the mould was pressed at 5 tons for 3 minutes. Then the mould was cooled down and composites were collected. The fibre content is shown in Table 3.3.

Two more composites, denoted as TPCA and TPCB, were made with the same method as making PCA and PCB, but using NaOH treated fibre mats as reinforcement. Their fibre contents can be seen in Table 3.3 as well.

A 100g pure PLA control specimen was also produced using the same procedures as above.

**Table 3.3 Fibre Content of PLA Powder/ CFF Mat Composites.**

| Composites | Amount of PLA powder | Amount of CFF mats | Fibre content wt% |
|---|---|---|---|
| PCA | 100g | 4 layers (9g) | 8% |
| PCB | 100g | 8 layers (18g) | 15% |
| PCC | 101g | 16 layers (30g) | 23% |
| TPCA | 100g | 4 layers of treated mats(10g) | 9% |
| TPCB | 100g | 8 layers of treated mats(20g) | 16% |

# 3.9 Thermal Conductivity Measuring

Thermal conductivity of PLA and its composites was measured according to the ASTM C 518-04 standard test method for steady-state thermal transmission properties by means of the heat flow meter apparatus.

## 3.9.1 Apparatus

The configuration in Fig. 2.15-a was chosen as the reference to set up the measuring apparatus in current research. A schematic is shown in Fig. 3.6. The upper aluminium plate acted as cold plate, which is kept cold by radiation. The lower aluminium plate acted as hot plate, which was heated by a hotplate. One sample and a heat flux sensor were mounted between the two aluminium plates.

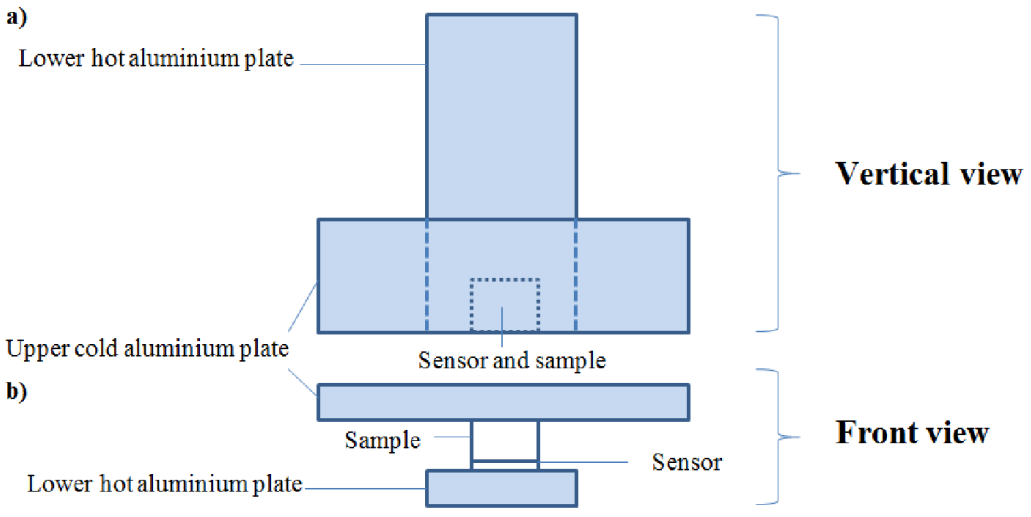


**Figure 3.6 Orthographic drawing of the Measuring Part, Showing a) Vertical and b) Front Projection.**

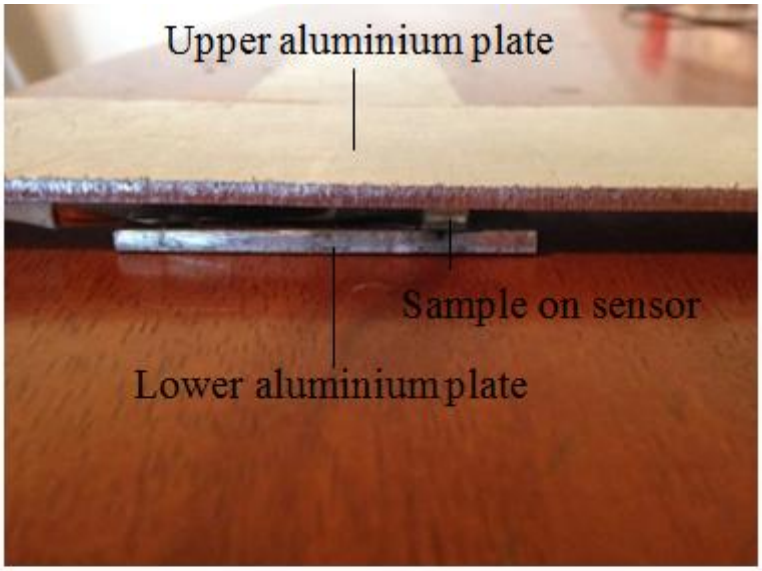


a

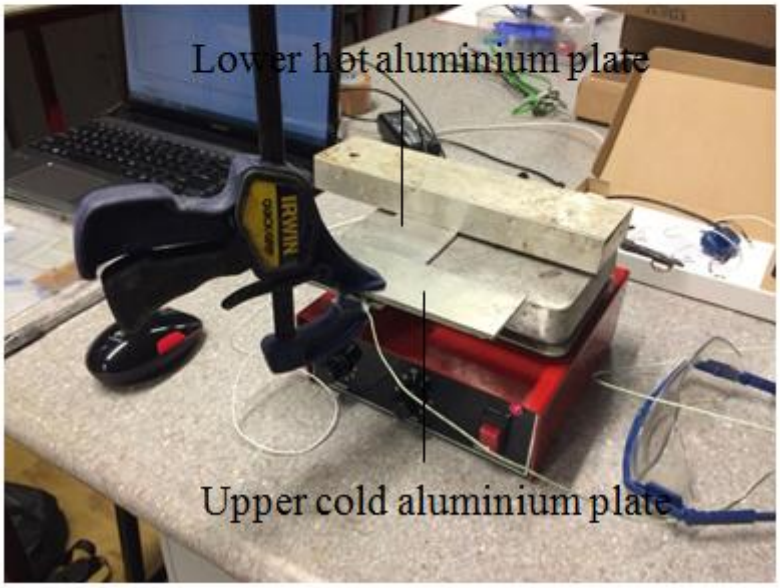


b

**Figure 3.7 Apparatus for Measuring Thermal Conductivity, a) Front View and b) Showing Equipment on Hot Plate.**

Pictures of the apparatus can be seen in Fig. 3.7. A gSKIN®-XB 27 9C heat flux sensor was mounted on the edge of an aluminium plate and then gSKIN® MOUNT-1212 thermal paste was used to attach a 5×5mm sample onto the measuring area of the heat flux sensor. Afterwards, another aluminium plate was placed on the top of the specimen with gSKIN® MOUNT-1212 thermal paste filling the gap between the specimen and the upper aluminium plate (Fig. 3.7b). A gSKIN® DLOG-4218 data logger was used to connect the heat flux sensor with a computer.

## 3.9.2 Data Collection

After the apparatus was set up, the hotplate was turned on to heat the lower aluminium plate. Analogue signals detected by the heat flux sensor were converted to digital data by gSKIN® DLOG-4218 data logger. MSR software was set according to section 3 of the instruction manual in appendix to output this digital signal. Sensitivity of the heat flux sensor used in current research was $1.7\mu V/(Wm^2)$. Signals from a K-type thermocouple were recorded by Pico® TC-08 data logger and could be read directly on a computer screen. The data at steady state (Fig. 3.8) were saved for further processing. Neat PLA, PCA, PCB and PCC samples were measured using this apparatus.

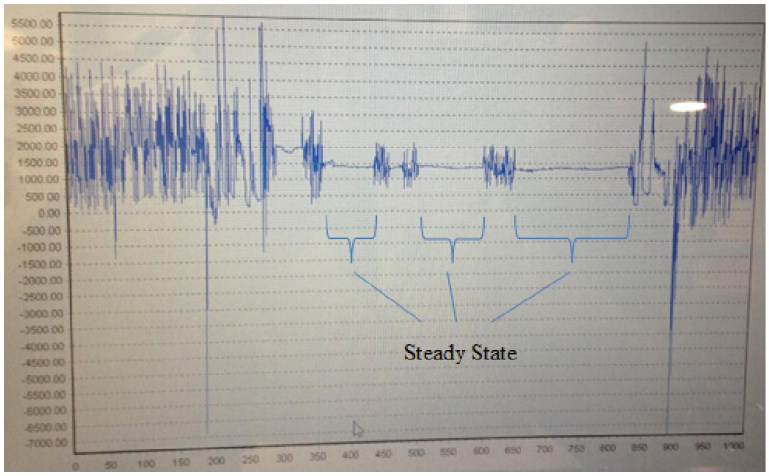


**Figure 3.8 Data Collected from Heat Flux Sensor**

## 3.10 Tensile Testing

Tensile testing was carried out according to the ASTM D 3039-08 Standard Test Method for Tensile Properties of Polymer Matrix Composite Materials. The specimens were tensile tested using an Instron-4202 tensile testing machine fitted with a 5 KN-load cell, operating at a rate of 2mm/min. Strain was measured with an Instron 2630-112 extensometer.

## 3.11 Scanning Electron Microscope

In the present research, composite fracture surface morphology was studied using an Hitachi S-4100 field emission scanning electron microscope.

# Chapter 4:

# Results and Discussion

# Chapter 4:

# Results and Discussion

## 4.1 Quality Analysis

### 4.1.1 CFF Mats

Experiments 1-6 in section 3.4 were carried out to assess the best value for swwl. The products of these experiments are shown in Fig 4.1.

The fibres stuck together to form a clump in Experiment 1, which can be seen in Fig. 4.1a. The left and right edges of the Kevlar holding sheet in Fig 4.1a were connected together before being removed from the sheet former cylinder. Therefore, the left clump and the top-right clump came from one piece. Clumping was due to lack of water on the surface of the holding material. Hence, fibres could not disperse freely to a uniform mat.

The product of Experiment 2 is shown in Fig. 4.1b. The fibre clump began to spread compared to the clumps in Experiment 1, though no sheet had been formed. The reason was that although increased water wall thickness had improved the flow of fibres, the improvement was not enough to form a uniform mat.

The product from experiment 3 was much improved forming almost a continuous mat (Fig. 4.1c). This indicated that a swwl value of 4 was getting closer to the optimized value for mat production. The detailed picture (Fig. 4.1e) shows the

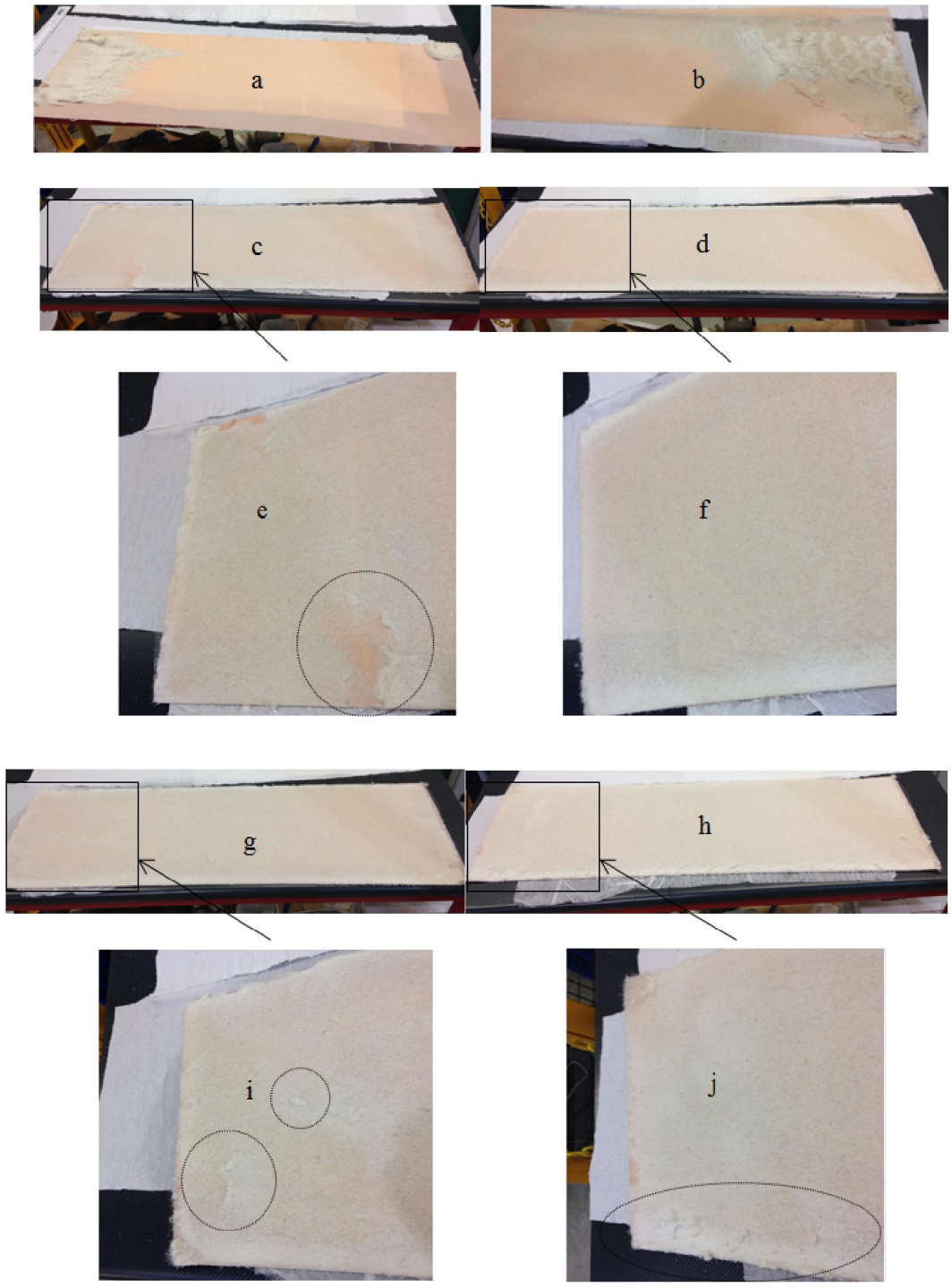


**Figure 4.1 a-the Product of Experiment 1, b- the Product of Experiment2, c-the Product of Experiment 3, d- the Product of Experiment 4, e-Detailed Picture for Picture c, f- Detailed Picture for Picture d, g-the Product of Experiment 5, h- the Product of Experiment 6, i-Detailed Picture for Picture g, j-Detailed Picture for Picture h.**

worst region (circled area) of the mat indicating that the level of water wall was not enough to spread fibres evenly.

The product from Experiment 4 with a swwl value of 5 was uniform with no apparent defects or fibre clumps.

The mats produced in Experiments 5 and 6 with swwl values of 6 and 8 respectively have relatively consistent texture (Fig. 4.1g and 4.1h), however, they had some small fibre clumps (see circled area in Fig. 4.1i and 4.1j). The reason is that the rotating speed of the sheet former cylinder could not provide enough centrifugal force to the water with thickness set in Experiments 5 and 6. Some fibres slowed down and stuck with others to form small clumps. In Experiment 6, some fibres even subsided to the bottom of the cylinder to form clumps, seen in Fig. 4.1j.

Based on Experiment 1-6, a value of swwl of 5 was selected.

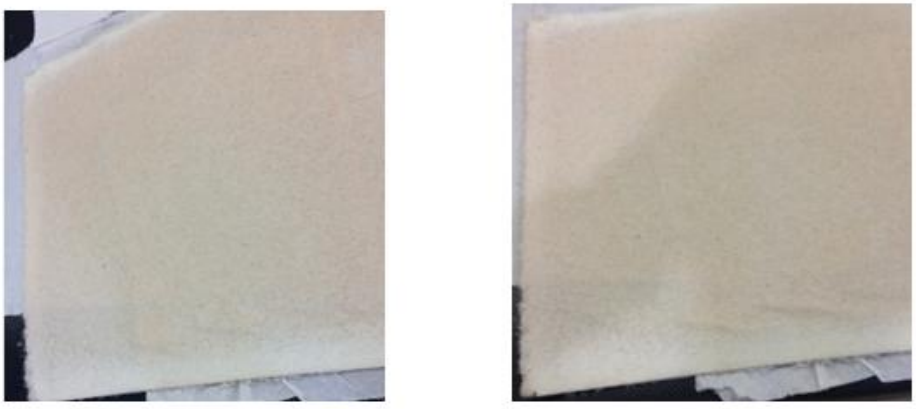

**Figure 4.2 The Product of Experiment 4 (left) and the Product of Experiment 7 (right).**

Experiment 7 was carried out to compare with Experiment 4 to assess the effect of pump value on quality of CFF mats. No apparent difference was found between

the mats of Experiment 7 and 4 (see Fig. 4.2). In Experiment 4, the mat was produced faster than that in Experiment 7 due to the higher pump value.

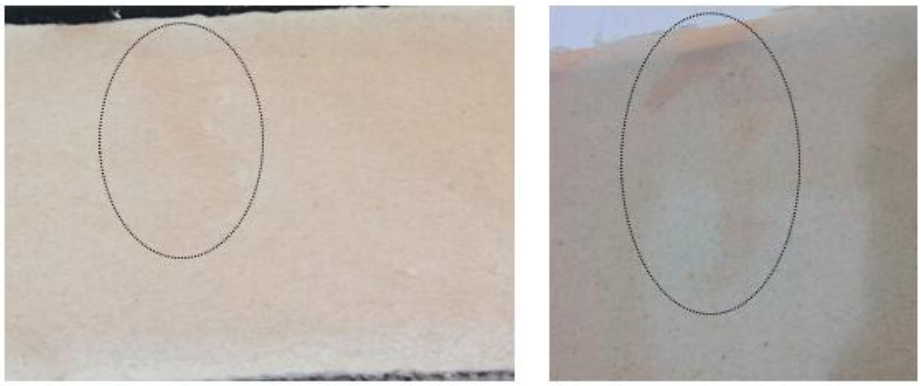

**Figure 4.3 The Product of Experiment 8 (left) and the Product of Experiment 9 (right).**

Experiments 8 and 9 explored the effects of feeding amount on quality of CFF mats. Fig. 4.3 left shows the product made from 25g CFFs; there was an area with less fibres than other parts of it. Fig. 4.3 right shows the product containing 15g CFFs which had a bigger defect area.

Overall, the products in Experiments 4 and 7 were most uniform, and with consideration of the efficiency, the parameter set in Experiment 4 was used to produce CFF mats for composites.

## 4.1.2 Composites


**Figure 4.4 Composite Specimen C4×2 Vertical View (left) and Lateral View (right).**

The initial consideration was to avoid PLA pellet penetrating and destroying CFF mats during hot press. Hence, PLA sheets were made to laminate with CFF mats. However, a poor wetting layer was observed after peeling off the outer PLA layer (Fig. 4.4). Although C4×2 was stable, the composites C8×2 broke along mats layers spontaneously (Fig. 4.5).

**Figure 4.5 Composite Specimen C8×2.**

Based on the results above, PLA powder was trialled for use in composite fabrication. The products showed better stability than those made from PLA sheets (Fig.4.6).

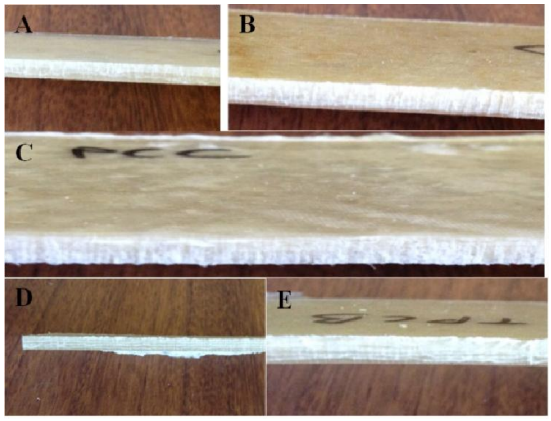


**Figure 4.6 Composite Specimens Made from PLA Powder A) PCA, B) PCB, C) PCC, D) TPCA, E) TPCB.**

## 4.2 Thermal Conductivity

According to ASTM C 518-04, data was collected at relatively steady state. Heat flow was read out from MSR 5.28.07 software, which can be seen in Fig. 4.7. The steady state heat flow, temperature difference and seperation between two plates for different specimens can be seen in Table 4.1.

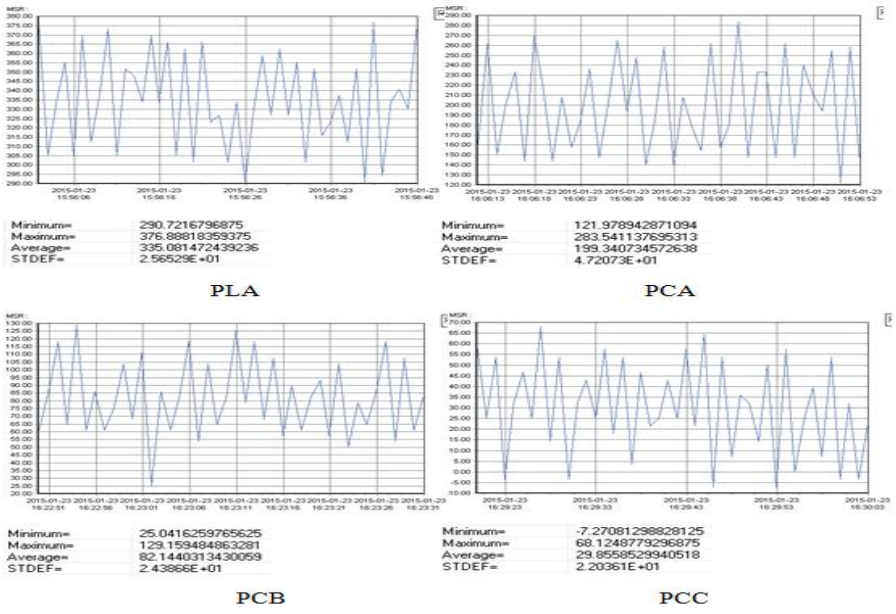


**Figure 4.7 Heat Flow Record at Steady State for Four Different Specimens.**

**Table 4.1 Steady State Heat Flow, Temperature Difference and Separation between Hot and Cold Plate.**

| Specimens | Heat flow ($W/m^2$) | Temperature difference (K) | Separation between hot and cold plate (m) |
|---|---|---|---|
| PLA | 335 | 16 | 0.0030 |
| PCA | 199 | 25 | 0.0030 |
| PCB | 82 | 18 | 0.0033 |
| PCC | 30 | 18 | 0.0040 |

According to ASTM C 518-04 section 8.2, thermal conductivity can be calculated using

$$\lambda = S \cdot E \cdot (\frac{L}{\Delta T}) \qquad 4\text{-}1$$

Where $\lambda$-thermal conductivity, $W/m \cdot K$

S-calibration factor of the heat flux transducer, $(W/m^2)/V$

E-heat flux transducer output, V

L-separation between the hot and cold plate assemblies during testing, m

$\Delta T$-temperature difference across the specimen, K

$S \cdot E$ is heat flow.

Thus, the thermal conductivity of specimens was calculated and shown in Table 4.2.

**Table 4.2 Thermal Conductivity of Specimens with Different Fibre Contents.**

| Specimens | Fibre content wt% | Thermal conductivity (W/m · K) |
|---|---|---|
| PLA | 0 | 0.063 |
| PCA | 8% | 0.024 |
| PCB | 15% | 0.015 |
| PCC | 23% | 0.007 |

Table 4.2 suggests that the thermal conductivity of composites reduced with increase in fibre content. The trend can be seen more clearly using a bar graph in Fig. 4.8. Composites with 8wt% CFF content had a thermal conductivity about 2.5 fold lower than that of pure PLA. After that, the decrease in thermal conductivity slowed down with an increase in CFF content.

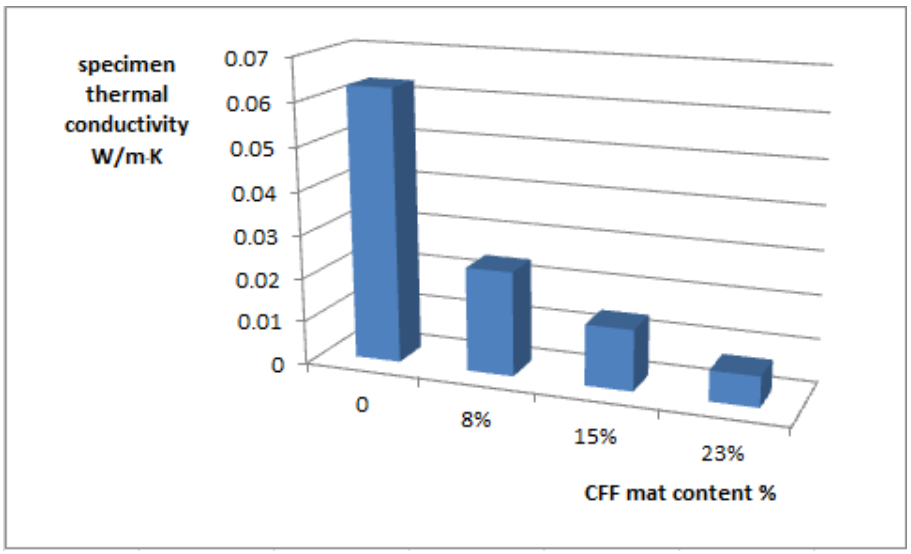


**Figure 4.8 Relation between Specimen Thermal Conductivity and CFF Content.**

The thermal conductivity of pure PLA was 0.063 W/m · K in Table 4.2, while the value in CES EduPack 2013 is 1.2-1.3 W/m · K. The measured value was

much smaller than the reference value, which can be explained as follows.

According to equation 4-1, S (calibration factor of the heat flux transducer) is a key parameter to a heat flux sensor. Essentially, a heat flux sensor is a thin chip comprising a thermopile and filling material (Fig. 4.13). It can only detect temperature difference between its two sides and produce an electric potential difference. For constantan/copper type thermopile, the electric potential difference detected is directly proportional to the temperature difference between hot and cold sides, which can be expressed by

$$E = f \cdot \Delta T$$

or

$$\Delta T = E/f \qquad 4\text{-}2$$

where, E is electric potential difference

$\Delta T$ is temperature difference between hot side and cold side

f is the coefficient of proportionality for this type thermopile.

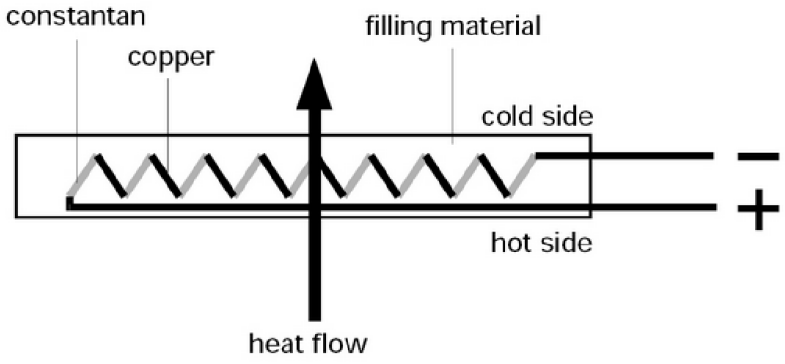


**Figure 4.9 Schematic of a Heat Flux Sensor [70].**

According to Fourier's Law, the heat flow through a heat flux sensor can be calculated as following,

$$q = k \cdot (\Delta T/\Delta x) \qquad 4\text{-}3$$

where, q is the heat flow

k is the thermal conductivity of the filling material

ΔT is temperature difference between hot side and cold side

Δx is the thickness of the heat flux sensor.

Use expression 4-2 to replace ΔT in equation 4-3, then equation 4-3 turns to be

$$q=（k\cdot E）/(f \cdot \Delta x)$$

besides q=S • E in equation 4-1, hence，

$$S= k/(f \cdot \Delta x) \qquad 4\text{-}4$$

The constants k and f will not change, but the thickness, Δx, will decrease because the sensor was frequently pressed by the sample and aluminium plates. This resulted in the increased value of S. Hence, the detected value of E would be smaller than real value and lead to a smaller value of thermal conductivity of specimens as supported by experimental data.

Although the measured thermal conductivity cannot be considered an absolute value, it still supports indication of a nine fold improvement in thermal insulation due to incorporating CFF mats into PLA.

# 4.3 Results of Tensile Testing and Discussion

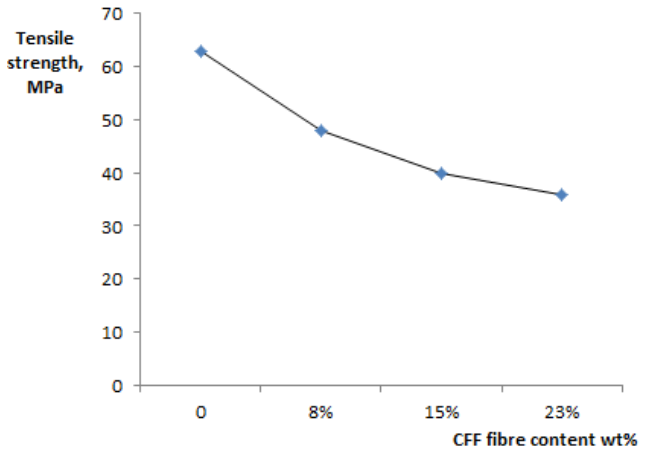


**Figure 4.10 Tensile Strength of PLA, PCA, PCB and PCC.**

Figure 4.10 displays the effect of untreated fibre content on tensile strength of PLA and composites produced with PLA powder. The tensile strength of samples decreased with increased untreated fibre content. This is a similar trend to that obtained from prior research of others [17]. The reason for the decrease in tensile strength is likely to be that the interfacial bonding between CFFs and PLA was weak.

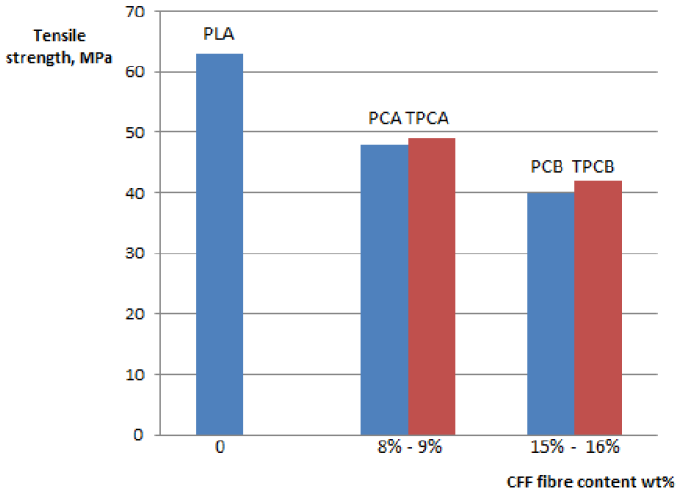


**Figure 4.11 Comparison of Tensile Strength between Different Specimens.**

Figure 4.11 compares the effect of alkali-treated fibre content on tensile strength of composites with the effect of untreated fibre content on tensile strength of composites. The tensile strength of samples decreased with increased alkali-treated fibre content, which was similar to the trend for untreated fibre composites. However, the decrease in tensile strength was slightly less (despite slightly higher fibre content ie. 9 and 16wt% for treated as opposed to 8 and 15wt% for untreated) by using alkali-treated fibres compared to using untreated fibres. This improvement is likely to be that the interfacial bonding between alkali-treated fibres and PLA was stronger than that between untreated fibres and PLA.

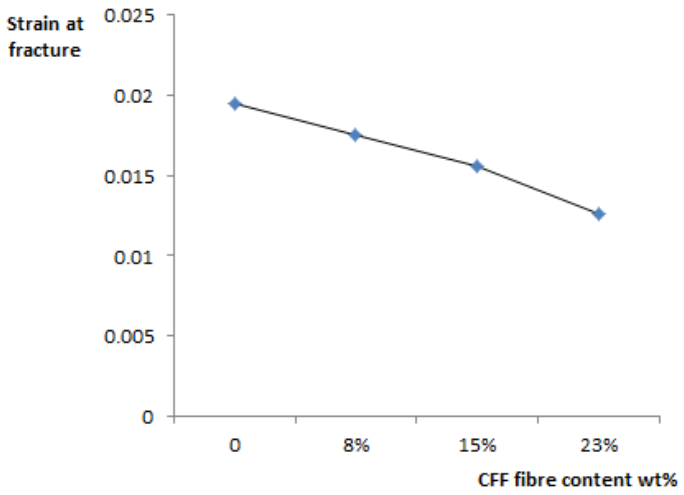


**Figure 4.12 Strain at Fracture of PLA, PCA, PCB and PCC.**

Figure 4.12 displays the effect of untreated fibre content on strain at fracture of PLA and composites produced with PLA powder. The strain at fracture of samples declined with increased untreated fibre content. The reason for the decline in strain at fracture is likely to be due to poor interfacial bonding between CFFs and PLA.

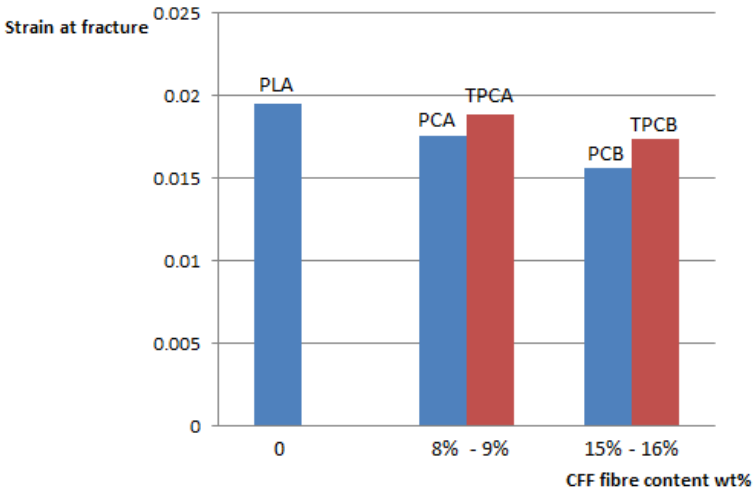


**Figure 4.13 Comparison of Strain at Fracture between Different Specimens.**

Figure 4.13 compares the effect of alkali-treated fibre content on strain at fracture of composites with the effect of untreated fibre content on stain at fracture of composites. The strain at fracture of samples decreased with increased alkali-treated fibre content, which was similar to the trend for untreated fibre composites. However, the decline in strain at fracture was less for using alkali-treated fibres compared to using untreated fibres. This improvement is likely to be due to the interfacial bonding between alkali-treated fibres and PLA being stronger than that between untreated fibres and PLA.

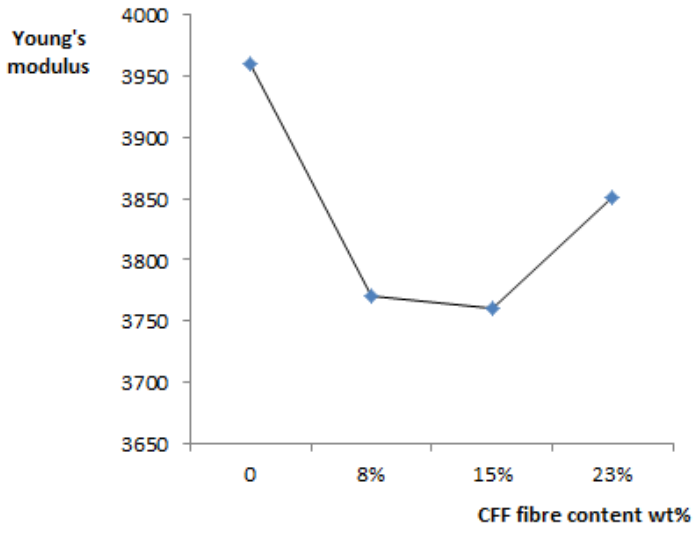


**Figure 4.14 Young's Modulus of PLA, PCA, PCB and PCC.**

Figure 4.14 shows the effect of untreated fibre content on Young's modulus of PLA and composites produced with PLA powder. The Young's modulus of samples decreased with an increase in untreated fibre content up to a fibre content of 15wt%, and then increased slightly when untreated fibre content rose up to 23wt%. The reason for the decrease in Young's modulus is likely to be due to poor interfacial bonding between CFFs and PLA.

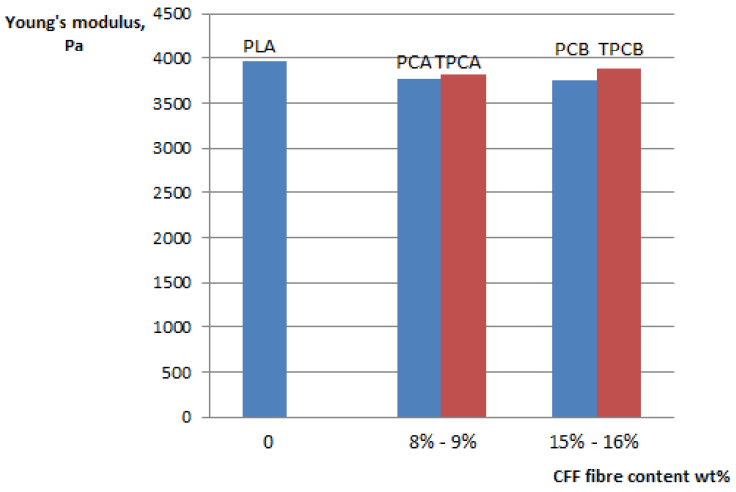


**Figure 4.15 Comparison of Young's Modulus between Different Specimens.**

Figure 4.15 compares the effect of alkali-treated fibre content on Young's modulus of composites with the effect of untreated fibre content on Young's modulus of composites up to a fibre content of 16%. The Young's modulus of samples decreased with increased alkali-treated fibre content, which was similar to the trend for untreated fibre composites. However, the decline in Young's modulus was less by using alkali-treated fibres compared to using untreated fibres. This improvement is likely to be that the interfacial bonding between alkali-treated fibres and PLA was better than that between untreated fibres and PLA.

# 4.4 SEM Results and Discussion

The SEM micrograph in Fig. 4.16 shows a fracture surface of PCA composite including the hollow structure of barbules. The SEM micrograph in Fig. 4.17 also shows the hollow structure of barbs in PCB sample. These hollow structures would entrap air and have contributed to the decrease in thermal conductivity of composites.

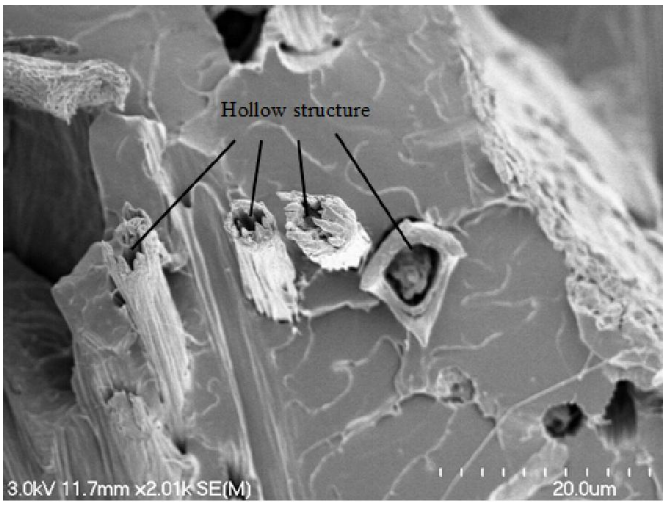


**Figure 4.16 PCA Fracture Surface SEM Picture ×2000**

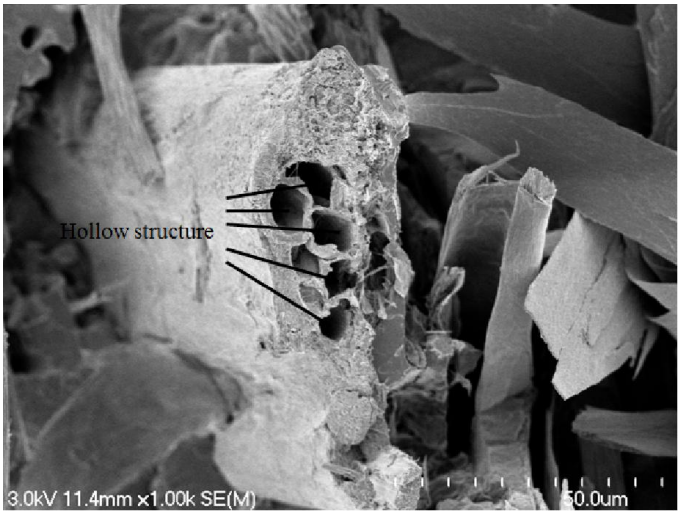


**Figure 4.17 PCB Fracture Surface SEM Picture ×1000**

The SEM micrograph in Fig. 4.18 exhibits a clear imprint from a barbule which has been pulled out from the matrix, which indicates a good degree of wetting (due to the matrix having followed the fibre contours). The SEM micrograph in Fig. 4.19 shows that a very limited number of barbules may have broken with the matrix (see circles in Fig. 4.19) instead of being pulled out. Generally, poor interfacial bonding is supported.

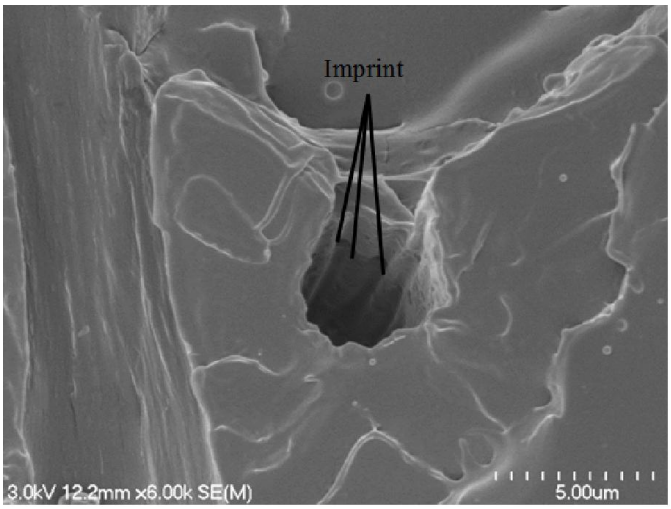


**Figure 4.18 PCB Fracture Surface SEM Picture ×6000**

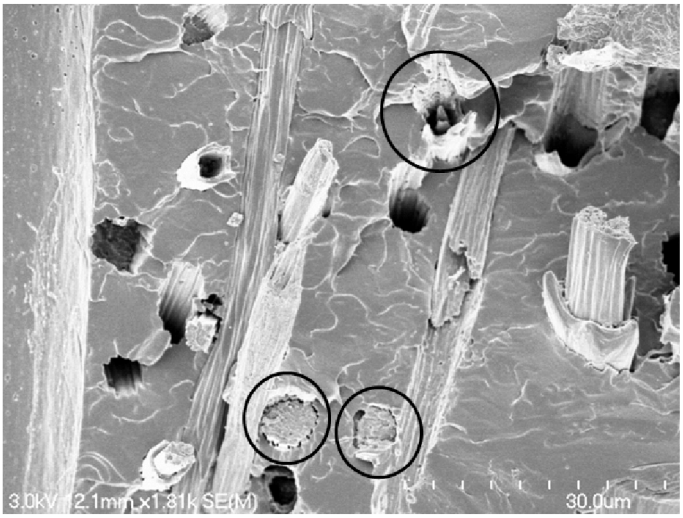


**Figure 4.19 PCB Fracture Surface SEM Picture ×500**

The circled areas in Fig. 4.20 suggest bad bonding between barbs and matrix. This explains the decrease in tensile strength for composites. The gaps between fibres and the matrix in Fig. 4.21 also suggest poor interfacial bonding which resulted in the decrease in tensile strength but contributed to the improvement in thermal insulation for composites.

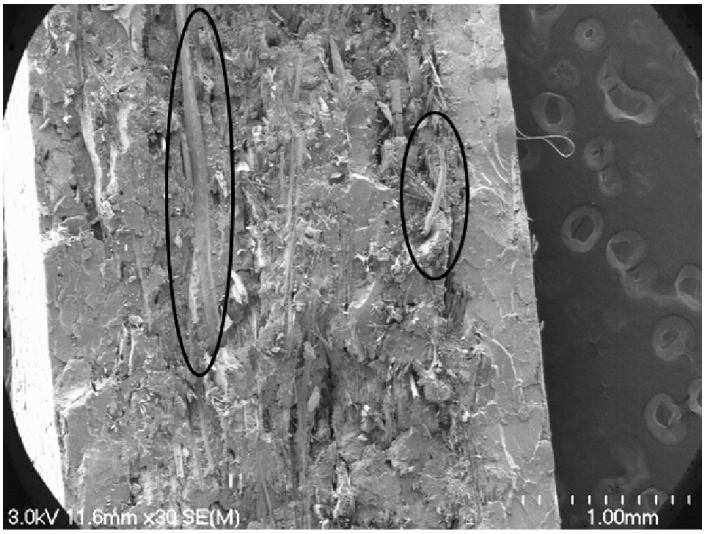


**Figure 4.20 PCB Fracture Surface SEM Picture ×30**

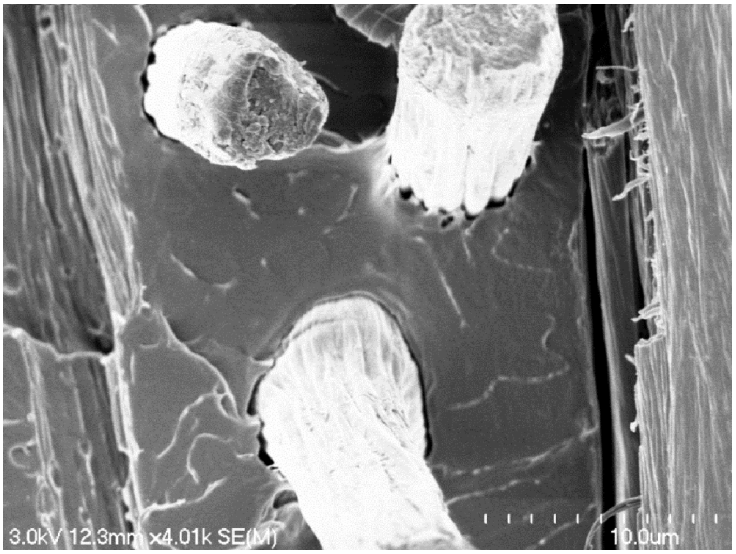


**Figure 4.21 PCB Fracture Surface SEM Picture ×4000**

# Chapter 5:

# Conclusions and Recommendations

# Chapter 5:

# Conclusions and Recommendations

## 5.1 Conclusions

An automatic dynamic sheet former is usually used to make paper with plant fibre pulp. Although chicken feather fibre has a lower density than water and is very soft compared to plant fibres, it turned out that uniform CFF mats could still be produced by the Canpa automatic dynamic sheet former. The uniformity of CFF mats was closely related to the water wall developed in the sheet former cylinder and the feeding amount of pulp. It was found that a swwl value of 5 and a feeding amount of at least 30g CFFs were the best condition for CFF mat production.

Composite specimens made with CFF mats and PLA sheet showed poor stability. The specimens containing 16 layers of mats broke spontaneously when handled. The samples containing 8 layers of mats could be pried open easily. Samples made of CFF mats and PLA powder were relatively stable; there was no obvious flaws on the cross sections seen when samples for testing were cut from composite sheets.

Results of tensile testing and SEM micrographs showed that samples made of PLA powder and CFF mats had poor interfacial bonding between fibres and the matrix. This poor interfacial bonding resulted in composites with worse tensile strength, lower failure strain and worse ductility than pure PLA. Results of tensile testing also indicated that alkali treatment of CFFs could improve the interfacial bonding between CFFs and the PLA matrix to a limited degree.

The heat flux meter method was found to be an unreliable long term method for measuring absolute thermal conductivity because the sensitivity of the heat flux sensor changed with time and needed to be calibrated regularly. However, relative thermal conductivity of samples was successfully obtained using the apparatus set up in current research. It was found that the thermal insulation of PLA was substantially improved by incorporating CFF mats into it. SEM analysis showed that the hollow structure of CFFs was maintained and so can have contributed to the improvement in thermal insulation. The poor interfacial bonding supported by mechanical testing and SEM could also have contributed to improved thermal insulation. Indeed, it is likely that there is a compromise between improving interfacial bonding for mechanical performance with the reduction of insulation this may bring about.

## 5.2 Recommendations

In the present research, CFF mats had been proved to be able to improve thermal insulation of PLA. However, the absolute value of thermal conductivity could not be measured using the apparatus in this research. In order to obtain the absolute value, the guarded hot plate method should be trialled in future research.

Alkali treatment of CFFs had been approved to be able to improve the interfacial bonding between CFFs and the PLA matrix in current research. Other methods such as using coupling agents and grafting polymers on CFFs should also be trialled in future research, although it should be considered that this may reduce performance with respect to thermal insulation.

Fabrication of CFFs and PLA fibre hybrid mats using ADSF should be explored to improve wetting of PLA into CFFs during composite production.

# References

# References


1. Strong, A. B. *Fundamentals of composites manufacturing: materials, methods, and applications*, 2nd edition; Society of Manufacturing Engineers: Dearborn, Michigan, 2008; p 5.
2. Yousif, B.F., et al., *Fracture behaviour of glass fibre-reinforced polyester composite.* Proceedings of the Institution of Mechanical Engineers, Part L: Journal of Materials: Design and Applications, 2009. 223(2): p. 83-89.
3. http://composite.about.com/od/aboutcarbon/a/Boeings-787-Dreamliner.htm
4. http://www.newscientist.com/article/dn7552-aviation--the-shape-of-wings-to-come.html?full=true#.U3vyFPmSwj4
5. Pervaiz, M. and M. M. Sain, *Carbon storage potential in natural fiber composites*. Resources, Conservation and Recycling, 2003, 39(4): p. 325-340.
6. http://www.lotuscars.com/gb/engineering/eco-elise
7. http://www.naturalfibersforautomotive.com/?cat=3
8. La Mantia, F.P. and M. Morreale, *Green composites: A brief review.* Composites Part A: Applied Science and Manufacturing, 2011. 42(6): p. 579-588.
9. Zini, E. and M. Scandola, *Green composites: An overview.* Polymer Composites, 2011, 32(12): 1905-1915.
10. Gareth Beckermanm., *The processing, production and improvement of hemp-fibre reinforced polypropylene composite materials*. 2004, Hamilton: the University of Waikato.
11. Ho, M. P., et al., *Critical factors on manufacturing process of natural fibre composites*. Composites Part B: Engineering, 2011(0).

12. Feughelman, M., Mechanical properties and structure of alpha-keratin fibres: wool, human hair, and related fibres. 1997, Sydney: University of New South Wales Press.
13. Tseng, F. J., *Biofibre production from chicken feather.* 2011, Hamilton: the University of Waikato.
14. Barone, J.R. and N.T. Gregoire, *Characterisation of fibre-polymer interactions and transcrystallinity in short keratin fibre-polypropylene composites.* Plastics Rubber and Composites, 2006. 35(6-7): p. 287-293.
15. Barone, J., W. Schmidt, and C. Liebner, *Compounding and molding of polyethylene composites reinforced with keratin feather fiber.* Composites Science and Technology, 2005. 65(3-4): p. 683-692.
16. http://web.a.ebscohost.com.ezproxy.waikato.ac.nz/ehost/detail?sid=5c0b62e8-97c5-4609-bc6f-f0b585ef3999%40sessionmgr4002&vid=3&hid=4101&bdata=JnNpdGU9ZWhvc3QtbGl2ZQ%3d%3d#db=bth&AN=84353987
17. Cheng, S., et al., *Mechanical and thermal properties of chicken feather fiber/PLA green composites.* Composites Part B-Engineering, 2009. 40(7): p. 650-654.
18. Callister, W. D., Jr., Rethwisch D. G. *Materials science and engineering: an introduction*, 8th edition; John Wiley and Sons, Inc: Hoboken, NJ, 2009; p 644.
19. Ye, W. and Broughton, M., R. *Chicken feather as a fibre source for nonwoven insulation.* International Nonwovens Journal, 1999. 8(1).
20. CES EduPack 2013
21. http://www.engineeringtoolbox.com/thermal-conductivity-d_429.html
22. http://www.corbion.com/bioplastics
23. http://www.corbion.com/bioplastics/markets/high-heat-packaging-disposables

24. Mors ter R.G., *Chicken feather fibre: A review.* 2013, Hamilton: the University of Waikato.
25. http://pianz.org.nz/industry-information/industry-statistics/poultry-production/meat-chicken-production
26. Bullions, T.A., et al., *Contributions of feather fibers and various cellulose fibers to the mechanical properties of polypropylene matrix composites.* Composites Science and Technology, 2006. 66(1): p. 102-114.
27. http://www.poultryhub.org/physiology/body-systems/integumentary-surface-of-the-bird/
28. http://www.answers.com/topic/feather-1
29. http://www.birds.cornell.edu/AllAboutBirds/studying/feathers/feathers
30. Huda, S. and Y. Yang, *Feather Fiber Reinforced Light-Weight Composites with Good Acoustic Properties.* Journal of Polymers and the Environment, 2009. 17(2): p. 131-142.
31. Reddy, N. and Y. Yang, *Structure and Properties of Chicken Feather Barbs as Natural Protein Fibers.* Journal of Polymers and the Environment, 2007. 15(2): p. 81-87.
32. Zhan, M. and R.P. Wool, *Mechanical properties of chicken feather fibers.* Polymer Composites, 2011. 32(6): p. 937-944.
33. Barone, J.R. and W.F. Schmidt, *Polyethylene reinforced with keratin fibers obtained from chicken feathers.* Composites Science and Technology, 2005. 65(2): p. 173-181.
34. Wool, R. P. and X. S. Sun, *Bio-based polymers and composites*, 1st ed.; Elsevier Academic Press: London, 2005.
35. Murayama-Arai K, T.R., Yokote Y, Akahane K, *Amino acid sequence of feather keratin from fowl.* Eur J Biochem, 1983. 132: p. 501-507.
36. Ganesh Sudalaiyandi, *Characterizing the cleaning process of chicken feathers*. 2012, Hamilton: the University of Waikato.

37. Dullaart R., *Keratin: Structure, properties, and application*. Nova Science Publishers: Hauppauge, NY, 2012; p 164.

38. Duh, B., *Reaction kinetics for solid-state polymerization of poly(ethylene terephthalate).* Journal of Applied Polymer Science, 2001. 81: p. 1748-1761.

39. Madhavan Nampoothiri, K., N.R. Nair, and R.P. John, *An overview of the recent developments in polylactide (PLA) research.* Bioresour Technol, 2010. 101(22): p. 8493-501.

40. Carothers, H.W., *Polymerization.* Chemical Reviews, 1931. 8(3): p. 353-426.

41. Guzman, J.D., R. Pollard, and J.D. Schieber, *Modeling of diffusion effects on step-growth polymerization.* Macromolecules, 2005. 38(1): p. 188-195.

42. Marcos-Gómez, D., et al., *Predicting the thermal conductivity of composite materials with imperfect interfaces.* Composites Science and Technology, 2010. 70(16): p. 2276-2283.

43. Agarwal, S., M.M.K. Khan, and R.K. Gupta, *Thermal conductivity of polymer nanocomposites made with carbon nanofibers.* Polymer Engineering and Science, 2008. 48(12): p. 2474.

44. Sanadi, A.R., et al., *Recycled newspaper fibers as reinforcing fillers in thermlplastics: Part I-Analysis of tensile and impact properties in polypropylene.* Journal of Reinforced Plastics and Composites, 1994. 13: p. 54-67.

45. Mwaikambo, L.Y. and M.P. Ansell, *Hemp fibre reinforced cashew nut shell liquid composites.* Composites Science and Technology, 2003. 63(9): p. 1297-1305.

46. Gassan, J. and A.K. Bledzki, *Alkali treatment of jute fibres: relationship between structure and mechanical properties.* Journal Of Applied Polymer Science, 1999. 71: p. 623-629.

47. Ghani, S.A., M.H. Jahari, and T. Soo-jin, *Effects of sodium hydroxide treatment on the properties of low-density polyethylene composites filled with chicken feather fiber.* Journal of Vinyl and Additive Technology, 2014. 20(1): p. 36-41.

48. Freddi, G., M. Tsukada, and H. Shiozaki, *Chemical modification of wool fibers with acid anhydrides.* Journal of Applied Polymer Science, 1999. 71: p. 1573-1579.

49. Martínez-Hernández, A.L., A.L. Santiago-Valtierra, and M.J. Alvarez-Ponce, *Chemical modification of keratin biofibres by graft polymerisation of methyl methacrylate using redox initiation.* Materials Research Innovations, 2008. 12(4): p. 184-191.

50. Mu, B. and P. Liu, *Surface Analysis of Polystyrene-Grafted Keratin Fiber via Surface-Initiated Atom Transfer Radical Polymerization.* Designed Monomers & Polymers, 2008. 11(1): p. 97-104.

51. Pickering, K.L., *The Effect of Poly[methylene(polyphenyl isocyanate)] and Maleated Polypropylene Coupling Agents on New Zealand Radiata Pine Fiber-Polypropylene Composites.* Journal of Reinforced Plastics and Composites, 2004. 23(18): p. 2011-2024.

52. Li, Y., *Effect of Coupling Agent Concentration, Fiber Content, and Size on Mechanical Properties of Wood/HDPE Composites.* International Journal of Polymeric Materials, 2012. 61(11): p. 882-890.

53. Koppel N., *Feather composites.* 2012, Hamilton: the University of Waikato.

54. Nishino, T., et al., *Kenaf reinforced biodegradable composite.* Composites Science and Technology, 2003. 63(9): p. 1281-1286.

55. Bos, H.L., J. Müssig, and M.J.A. van den Oever, *Mechanical properties of short-flax-fibre reinforced compounds.* Composites Part A: Applied Science and Manufacturing, 2006. 37(10): p. 1591-1604.

56. Michaeli, W., Kaufmann, H., Greif, H., and Vosseburger, F.-J., *Training In Plastics Technology*. 1995: Hanser Publishers.

57. Ben, G., et al., *Examination of heat resistant tensile properties and molding conditions of green composites composed of kenaf fibers and PLA resin.* Composite Mater., 2007. 16(4): p. 361-376.

58. http://www.nedians.8m.com/compression.htm

59. Wrzesniewska-Tosik, K., et al., *Fibrous composites based on keratin from chicken feathers.* Fibres & Textiles in Eastern Europe, 2011. 19(6 (89)): p. 118-123.

60. Fathi-Khalfbadam, S., et al., *Analysis and Simulation of Fiber Dispersion in Water Using a Theoretical Analogous Model.* Journal of Dispersion Science and Technology, 2011. 32(3): p. 352-358.

61. ASTM C177-04, Standard Test Method for Steady-State Heat Flux Measurements and Thermal Transmission Properties by Means of the Guarded-Hot-Plate Apparatus.

62. http://www.beal.co.nz/uploads/79343/files/The_Thermal_Conductivity_Test_Tool.pdf

63. ASTM C1114-00, Standard test method for steady-state thermal thransmission properties by means of the thin-heater apparatus.

64. ASTM C518-04, Standard test method for steady-state thermal transmission properties by means of the heat flow meter apparatus.

65. Al-Homoud, D.M.S., *Performance characteristics and practical applications of common building thermal insulation materials.* Building and Environment, 2005. 40(3): p. 353-366.

66. Carus, M., *Increasing demand for european hemp fibres: A sustainable raw material for bio-based composites.* 2010.

67. Liu, D., et al., *Manufacturing of a biocomposite with both thermal and acoustic properties.* Journal of Composite Materials, 2012. 46(9): p. 1011-1020.

68. Takagi, H., et al., *Thermal conductivity of PLA-bamboo fiber composites.* Composite Mater., 2007. 16(4): p. 377-384.

69. Ghani, S.A., M.H. Jahari, and T. Soo-jin, *Effects of sodium hydroxide treatment on the properties of low-density polyethylene composites filled with chicken feather fiber.* Journal of Vinyl and Additive Technology, 2014. 20(1): p. 36-41.

70. http://cnx.org/contents/18a61cb9-75db-486d-b3c4-40e3181e1c13@1.1:2/Body_Ambient_Bondgraph_Model_U

71. Carson, J.K. and J.P. Sekhon, *Simple determination of the thermal conductivity of the solid phase of particulate materials.* International Communications in Heat and Mass Transfer, 2010. 37(9): p. 1226-1229.

72. Behzad, T. and M. Sain, *Measurement and prediction of thermal conductivity for hemp fiber reinforced composites.* Polymer Engineering and Science, 2007. 47(7): p. 977.

# Appendix

gSKIN®

# Instruction Manual

for

# gSKIN® DLOG Data Logger

greenTEG AG

Technoparkstrasse 1
8005 Zürich, Switzerland

T: +41 44 632 04 20
F: +41 44 632 14 62

info@greenTEG.com
greenTEG.com

## 1. Package content

1 gSKIN® DLOG Data Logger
1 USB cable (PC to data logger)
1 installation CD for read-out software

## 2. Requirements

The read-out software needs to be installed on the computer used for adjusting the data logger settings. In order to change settings of the data logger, it needs to be connected to the PC via the USB cable.

## 3. Changing the measurement unit

The data logger can record your measurements either in voltage (V), heat flux (W/m$^2$) or power (W). By default, the data logger is set to record heat flux (W/m$^2$).

In order to change the measurement unit, follow these instructions:

1. Connect the data logger to the PC.
2. Open the software.
3. Figure 1 shows the start screen.

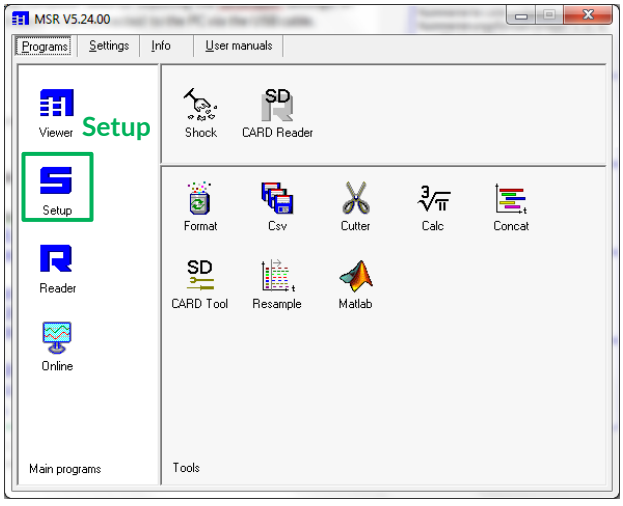


*Figure 1: Start screen of read-out software*

4. In the **Setup** section (see Figure 2) of the read-out software, choose the tab **User settings.**
5. If multiple data loggers are connected, first choose the data logger for which you want to change the settings.

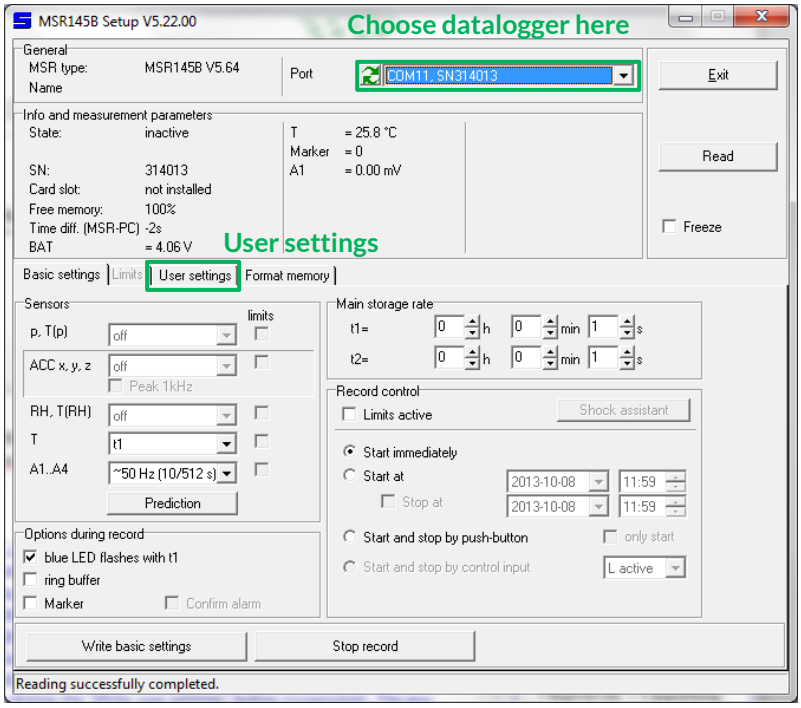


*Figure 2: Setup dialog*

6. Click the **Calibrate** button in the **Analog inputs** box shown in Figure 3. The window shown in Figure 4 will pop up.

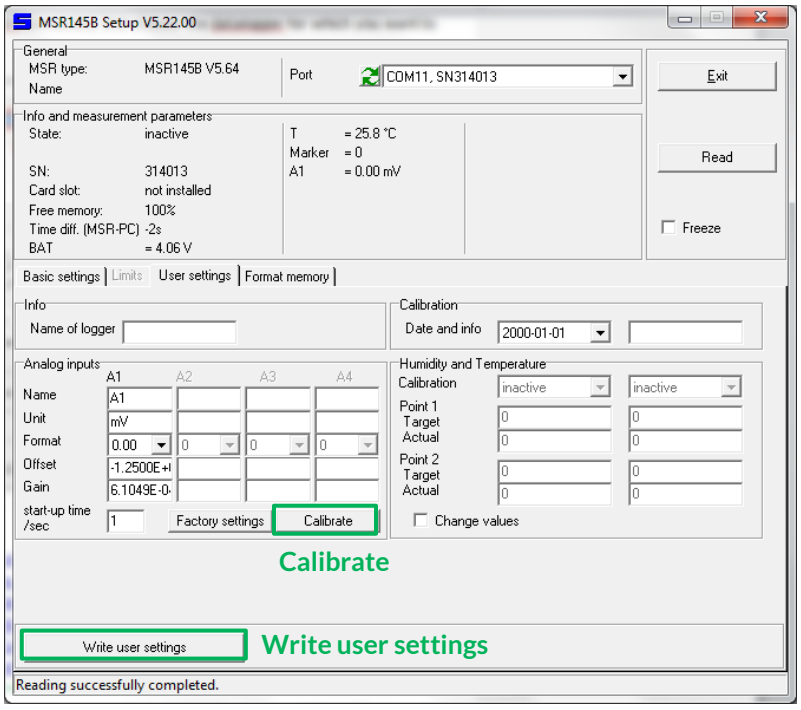


*Figure 1: User settings dialog*

7. In the "Analog inputs" window, overwrite the current target values according to Table 1.

*Explanatory note:* The data logger carries out an analog digital conversion (ADC) of the sensor input. The 12-bit resolution leads to a total of 4095 digital levels, which correspond to the voltage input of the sensor. In the **Calibration** window, a two point calibration is done by defining target values for specific digital levels (ADC value). Typically, the target values for the center level (ADC 2047) and the highest value (ADC 4095) are used.

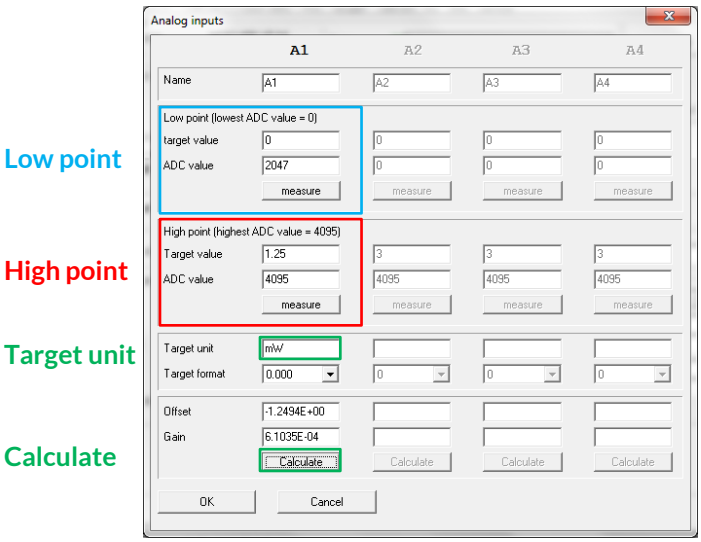


*Figure 4: Window used for input of gSKIN calibration values*

The output signal of the gSKIN® Sensor is a voltage. In order to get the values for the recorded heat flux in W/m$^2$, the sensitivity S of the sensor needs to be included in the field "Target value" of the "High point". Please calculate this value by using the formula in the corresponding field in Table 1. You find the respective constant S for your gSKIN® Sensor in the delivered calibration protocol. To obtain the incident power in W, the value S needs to be divided by the area A of the sensor. The other fields do not need any calculation.

Table 1 lists the values that should be entered into the window shown in Figure 4. The values depending on the data logger model you are using.

| | | gSKIN® DLOG-4217 | | gSKIN® DLOG-4218 | | gSKIN® DLOG-4219 | |
|---|---|---|---|---|---|---|---|
| | | mV | W/m$^2$<br>W | mV | W/m$^2$<br>W | mV | W/m$^2$<br>W |
| Low point | Target value | 0 | 0 | 0 | 0 | 0 | 0 |
| | ADC value | 2047 | 2047 | 2047 | 2047 | 2047 | 2047 |
| High point | Target value | 62.5 | 0.0625/S<br>0.0625/(S/A) | 12.5 | 0.0125/S<br>0.0125/(S/A) | 1.25 | 0.00125/S<br>0.00125/(S/A) |
| | ADC value | 4095 | 4095 | 4095 | 4095 | 4095 | 4095 |

*Table 1: List of calibration values for gSKIN® DLOG-4217, DLOG-4218 and DLOG-4219*

8. Adapt the target unit according to the measurement unit desired. You can determine the format of the recorded data in the field target format.

**Examples:**

1. gSKIN® DLOG-4217 with a gSKIN® Sensor sensitivity of S = 2 µV/(W/m$^2$) set to W/m$^2$.
    a. In the fields of the **Low point** (see Figure 4), enter the following values:
        i. Target value: 0
        ii. ADC value: 2047
    b. In the fields of the **High point**, enter:
        i. Target value: 0.0625/0.000002 = 31 250
        ii. ADC value: 4095
    c. Change the **Target unit** to W/m$^2$.

2. gSKIN® DLOG-4219 with a gSKIN® Sensor sensitivity of 2 µV/(W/m$^2$) set to mW.
    a. In the fields of the **Low point** (see Figure 4), enter the following values:
        i. Target value: 0
        ii. ADC value: 2047
    b. In the fields of the **High point**, enter:
        i. Target value: 0.00125/(0.000002/(0.0085*0.0085))*1000= 45.1
        ii. ADC value: 4095
    c. Change the **Target unit** to mW.

9. Adapt the target unit according to the measurement unit desired. You can determine the format of the recorded data in the field target format.
10. Calculate the offset and gain by clicking the **Calculate** button. This will determine the parameters, which are used by the software to transform the ADC scale into the units you have entered (i.e. mV, W/m$^2$ or W).
11. Click **OK** to save the new settings and to return to the User settings dialog.
12. Activate the new settings by clicking the **Write user settings** button (see Figure 3). The new settings are now written to the data logger and will be applied to all acquired data.
13. Return to the start screen of the read-out software by clicking **Exit**.
14. Continue/Start your measurements.

## Disclaimer

The above restrictions, recommendations, materials, etc. do not cover all possible cases and items. This document is not to be considered to be complete and it is subject to change without prior notice.

## Revision History

| Date | Revision | Changes |
|---|---|---|
| 11. November 2013 | 0.1 (preliminary) | Initial revision |